

Electronic Supporting Information

Cationic Magnesium Hydride [MgH]⁺ Stabilized by an NNNN-Type Macrocycle

L. E. Lemmerz,^a D. Mukherjee,^{a,b} T. P. Spaniol,^a A. Wong,^c G. Ménard,^c L. Maron^d and J. Okuda*^a

^aInstitute of Inorganic Chemistry, RWTH Aachen University, Landoltweg 1, 52056 Aachen, Germany

^bDepartment of Chemistry, Indian Institute of Technology Kharagpur, Kharagpur 721302, West Bengal, India

^cDepartment of Chemistry and Biochemistry, University of California, Santa Barbara, California, 93106, USA

^d CNRS, INSA, UPS, UMR 5215, LPCNO, Université de Toulouse, 135 avenue de Rangueil, 31077 Toulouse, France

Table of Contents

General considerations	S1
Synthesis of [(Me ₄ TACD)Mg(μ-H) ₂ Mg(HMDS) ₂] (1)	S2
¹ H, ¹³ C{ ¹ H} and ²⁹ Si{ ¹ H} NMR of [(Me ₄ TACD)Mg(μ-H) ₂ Mg(HMDS) ₂] (1)	S2
Synthesis of [(Me ₄ TACD)Mg(μ-D) ₂ Mg(HMDS) ₂] (1-d₂)	S4
¹ H, ² D, ¹³ C{ ¹ H} and ²⁹ Si{ ¹ H} NMR of [(Me ₄ TACD)Mg(μ-D) ₂ Mg(HMDS) ₂] (1-d₂)	S4
Synthesis of [(Me ₄ TACD) ₂ Mg ₂ (μ-H) ₂][B(3,5-Me ₂ -C ₆ H ₃) ₄] ₂ (2)	S6
¹ H, ¹³ C{ ¹ H} and ¹¹ B{ ¹ H} NMR of [(Me ₄ TACD) ₂ Mg ₂ (μ-H) ₂][B(3,5-Me ₂ -C ₆ H ₃) ₄] ₂ (2)	S7
Synthesis of [(Me ₄ TACD) ₂ Mg ₂ (μ-D) ₂][B(3,5-Me ₂ -C ₆ H ₃) ₄] ₂ (2-d₂)	S9
¹ H, ² D, ¹³ C{ ¹ H} and ¹¹ B{ ¹ H} NMR of [(Me ₄ TACD) ₂ Mg ₂ (μ-D) ₂][B(3,5-Me ₂ -C ₆ H ₃) ₄] ₂ (2-d₂)	S9
Synthesis of [(Me ₄ TACD)Mg(μ-H) ₃ BH][B(3,5-Me ₂ -C ₆ H ₃) ₄] (3)	S11
¹ H, ¹³ C{ ¹ H} and ¹¹ B NMR of [(Me ₄ TACD)Mg(μ-H) ₃ BH][B(3,5-Me ₂ -C ₆ H ₃) ₄] (3)	S12
Synthesis of [(Me ₄ TACD)Mg(μ-H)BHpin][B(3,5-Me ₂ -C ₆ H ₃) ₄] (4)	S14
¹ H, ¹³ C{ ¹ H}-APT and ¹¹ B NMR of [(Me ₄ TACD)Mg(μ-H)BHpin][B(3,5-Me ₂ -C ₆ H ₃) ₄] (4)	S15

Solid state structure of [(Me ₄ TACD)Mg(μ-H)BHpin)][B(3,5-Me ₂ -C ₆ H ₃) ₄] (4)	S16
Synthesis of [(Me ₄ TACD)Mg(H ₂ Al ^t Bu ₂)][B(3,5-Me ₂ -C ₆ H ₃) ₄] (5)	S17
¹ H, ¹³ C{ ¹ H}, ²⁷ Al and ¹¹ B{ ¹ H} NMR of [(Me ₄ TACD)Mg(H ₂ Al ^t Bu ₂)][B(3,5-Me ₂ -C ₆ H ₃) ₄] (5)	S18
Synthesis of [(Me ₄ TACD)Mg(OCH ₂ Ph)][B(3,5-Me ₂ -C ₆ H ₃) ₄] (6)	S20
¹ H, ¹³ C{ ¹ H} and ¹¹ B{ ¹ H} NMR of [(Me ₄ TACD)Mg(OCH ₂ Ph)][B(3,5-Me ₂ -C ₆ H ₃) ₄] (6)	S21
Synthesis of [(Me ₄ TACD)Mg(OCHPh ₂)][B(3,5-Me ₂ -C ₆ H ₃) ₄] (7)	S23
¹ H, ¹³ C{ ¹ H} and ¹¹ B{ ¹ H} NMR of [(Me ₄ TACD)Mg(OCHPh ₂)][B(3,5-Me ₂ -C ₆ H ₃) ₄] (7)	S24
Synthesis of [(Me ₄ TACD)Mg(1,2-DHP)][B(3,5-Me ₂ -C ₆ H ₃) ₄] (8a)	S25
¹ H, ¹³ C{ ¹ H} and ¹¹ B{ ¹ H} NMR of [(Me ₄ TACD)Mg(1,2-DHP)][B(3,5-Me ₂ -C ₆ H ₃) ₄] (8a)	S26
Synthesis of [(Me ₄ TACD)Mg(1,4-DHP)][B(3,5-Me ₂ -C ₆ H ₃) ₄] (8b)	S28
¹ H, ¹³ C{ ¹ H} and ¹¹ B{ ¹ H} NMR of [(Me ₄ TACD)Mg(1,4-DHP)][B(3,5-Me ₂ -C ₆ H ₃) ₄] (8b)	S29
Synthesis of [Mg(THF) ₆][B(3,5-Me ₂ -C ₆ H ₃) ₄] ₂ (9)	S30
¹ H, ¹³ C{ ¹ H} and ¹¹ B{ ¹ H} NMR of [Mg(THF) ₆][B(3,5-Me ₂ -C ₆ H ₃) ₄] ₂ (9)	S31
Solid state structure of [Mg(THF) ₆][B(3,5-Me ₂ -C ₆ H ₃) ₄] ₂ (9)	S32
Isomerization of 8a into 8b in the presents of 9 in THF- <i>d</i> ₈ at 70 °C	S33
Exchange reactions of 8a and 8b in pyridine- <i>d</i> ₅	S34
Crystal Structure Determinations	S36
DFT Calculations	S40
References	S44

General considerations

All operations were performed under inert atmosphere of dry argon using standard Schlenk techniques or glovebox techniques. THF, THP, Et₂O, *n*-pentane, *n*-hexane and toluene were purified using a MB SPS-800 solvent purification system or distilled under argon from sodium/benzophenone ketyl prior to use. Pyridine was dried over CaH₂ and distilled under argon prior to use. Deuterated solvents (THF-*d*₈, benzene-*d*₆) were distilled under argon from sodium/benzophenone ketyl prior to use. The starting materials Me₄TACD^[1] and [NEt₃H][B(3,5-Me₂-C₆H₃)₄]^[2] were prepared according to literature procedures. The starting material [Mg(HMDS)₂(THF)₂] were analogously prepared to [Mg(HMDS)₂(OEt)₂].^[3] NMR spectra were recorded on a Bruker Avance II 400 or a Bruker Avance III HD 400 spectrometer at 25 °C in J. Young-type NMR tubes. Chemical shifts (δ in ppm) in the ¹H, ¹³C{¹H} and ²⁹Si{¹H} NMR spectra were referenced to the residual proton signals of the deuterated solvents and reported relative to tetramethylsilane. The resonances in the ¹H and ¹³C NMR spectra were assigned on the basis of two-dimensional NMR experiments (COSY, HSQC, HMBC). Combustion analyses were performed with an Elementar Vario EL. The low carbon content for **3**, **4**, **6**, **8a** and **8b** may be ascribed to incomplete combustion.^[4] The magnesium contents were determined by complexometric titrations and were carried out according to the published procedure^[5] or were determined by inductively coupled plasma mass spectrometry using a Spectro ICP Spectroflame D instrument. A defined amount of sample was dissolved in 8 mL of 40% hydrofluoric acid, 2 mL of concentrated sulfuric acid, and 40 mL of water.

[(Me₄TACD)Mg(μ-H)₂Mg(HMDS)₂] (1). A solution of Me₄TACD (114 mg, 0.5 mmol) and PhSiH₃ (216 mg, 2.0 mmol) in toluene (2mL) was added slowly to a solution of [Mg(HMDS)₂(THF)₂] (489 mg, 1.0 mmol) in toluene (2mL). The reaction mixture was left for 3 days at 25 °C and the product crystallized during that time. The mother liquor was decanted off. The crystals were washed with *n*-pentane (3 x 3 mL) and dried under reduced pressure to give [(Me₄TACD)Mg(μ-H)₂Mg(HMDS)₂] (1) (247 mg, 0.41 mmol) as slightly yellow crystals; yield: 82%. Single crystals suitable for X-ray analysis were obtained from toluene over a period of 72 h. ¹H NMR (THF-*d*₈; 400.1 MHz): δ 0.05 (s, 36H, N{Si(CH₃)₃}), 2.58 (s, 12H, CH₃-Me₄TACD), 2.65 - 2.72 (m, 8H, CH₂-Me₄TACD), 2.75 - 2.82 (m, 8H, CH₂-Me₄TACD), 3.61 (s, 2H, MgH₂) ppm. ¹³C{¹H} NMR (THF-*d*₈; 100.6 MHz): δ 7.67 (N{Si(CH₃)₃}₂), 47.1 (CH₃-Me₄TACD), 56.4 (CH₂-Me₄TACD) ppm. ²⁹Si{¹H} NMR (THF-*d*₈; 79.5 MHz): δ -11.32 ppm. Anal. calc. for C₂₄H₆₆N₆Si₄Mg₂ (566.78 g·mol⁻¹): C, 48.06; H, 11.09; N, 14.01; Mg, 8.10. Found: C, 47.30; H, 10.71; N, 14.05; Mg, 8.35%.

¹H, ¹³C{¹H} and ²⁹Si NMR spectra of [(Me₄TACD)Mg(μ-H)₂Mg(HMDS)₂] (1)

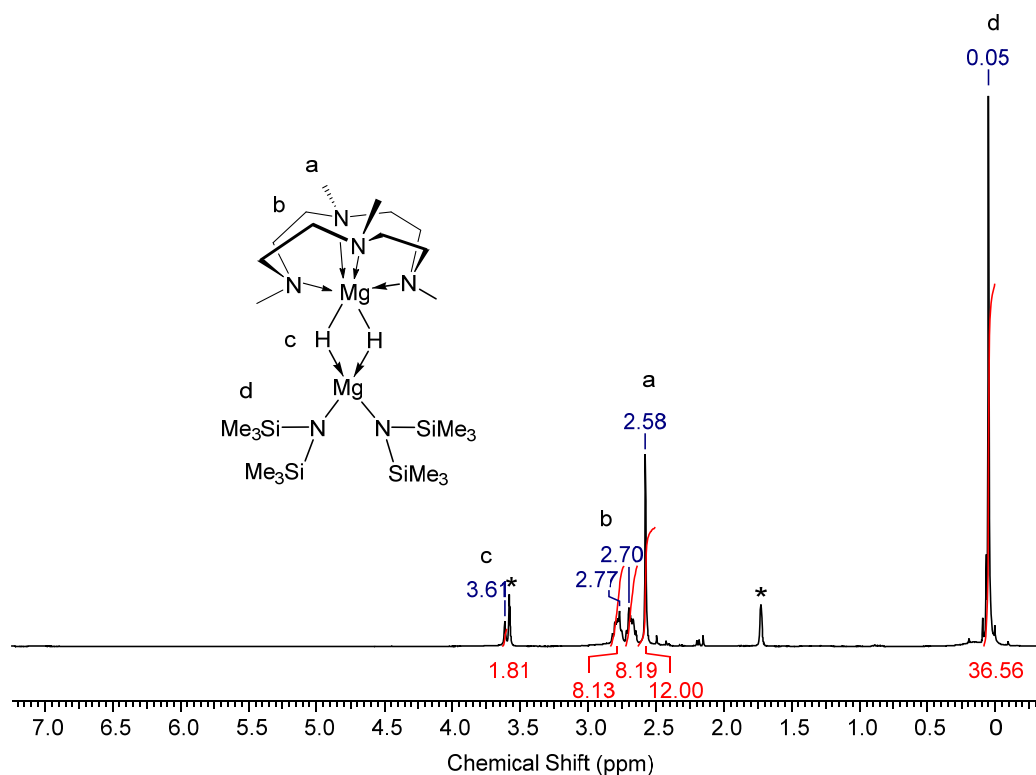


Figure S1. ¹H NMR spectrum of **1** in THF-*d*₈ (*) at 25 °C.

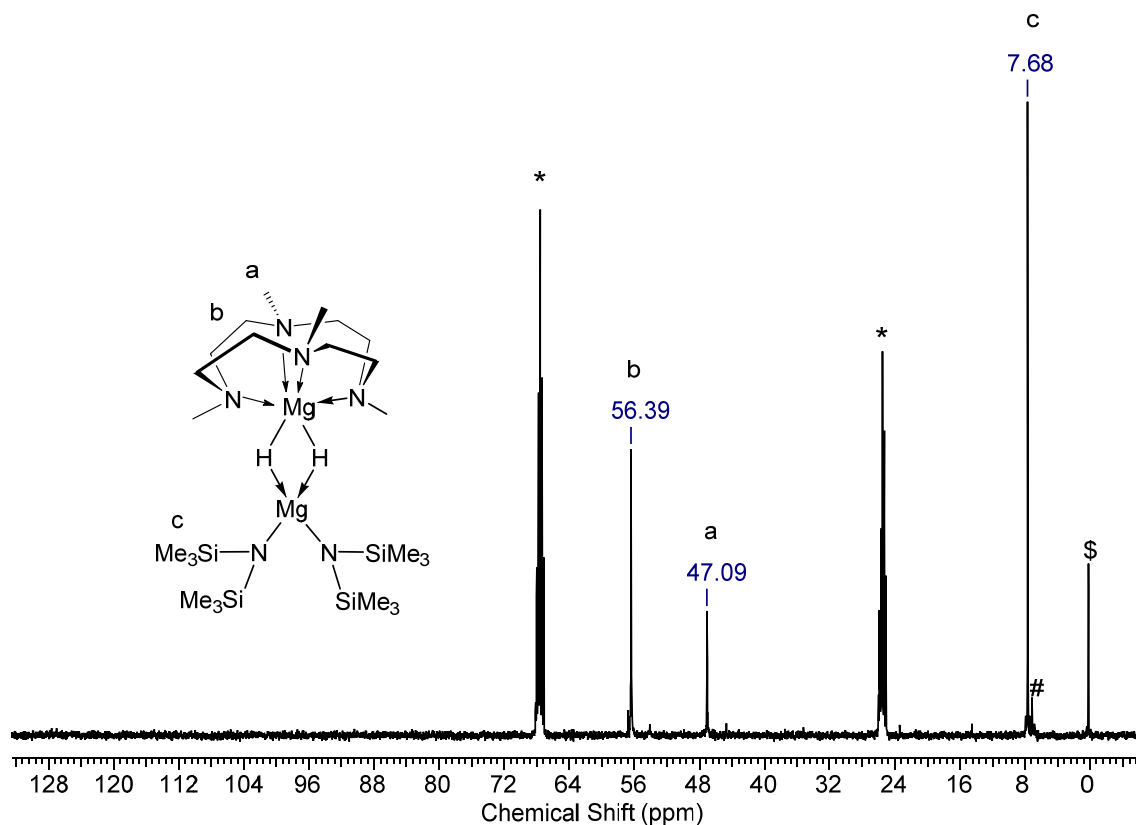


Figure S2. $^{13}\text{C}\{^1\text{H}\}$ NMR spectrum of **1** in $\text{THF-}d_8$ (*) at $25\text{ }^\circ\text{C}$ (# unidentified species, \$ TMS).

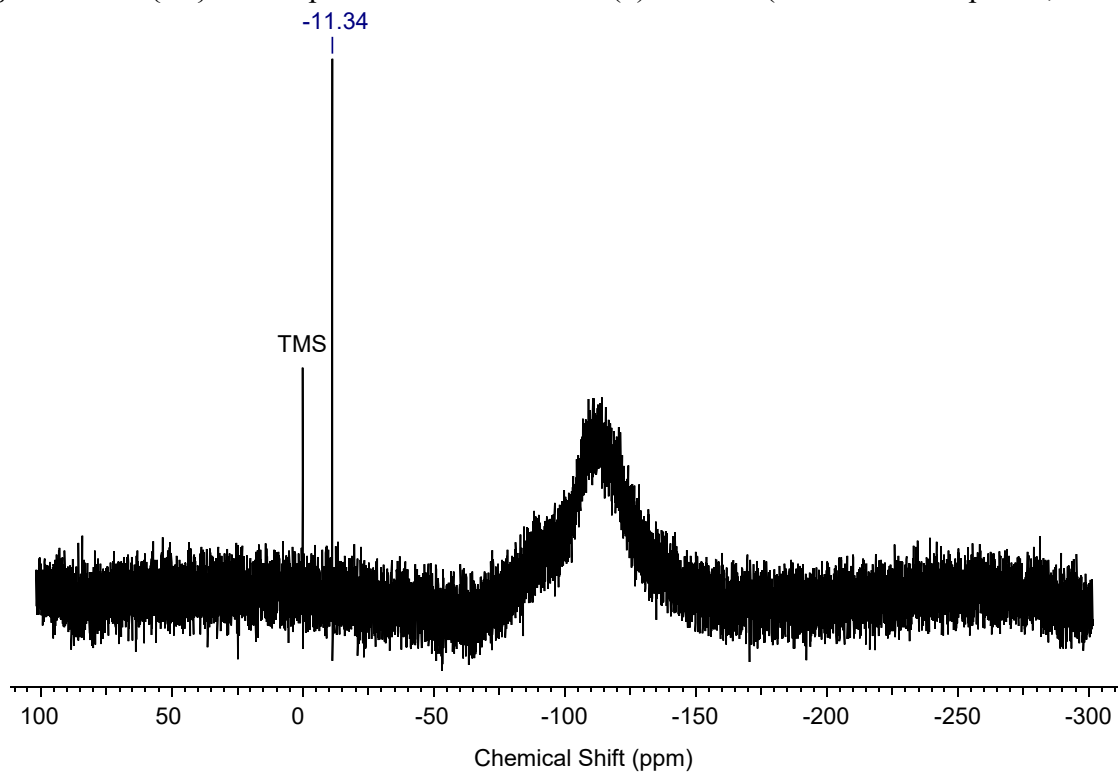


Figure S3. $^{29}\text{Si}\{^1\text{H}\}$ NMR spectrum of **1** in $\text{THF-}d_8$ at $25\text{ }^\circ\text{C}$.

[(Me₄TACD)Mg(μ-D)₂Mg(HMDS)₂] (1-d₂). A solution of Me₄TACD (46 mg, 0.2 mmol) and PhSiD₃^[6] (89 mg, 0.8 mmol) in toluene (2mL) was added slowly to a solution of [Mg(HMDS)₂(THF)₂] (196 mg, 1.0 mmol) in toluene (2mL). The reaction mixture was left for 3 days at 25 °C and the product crystallized during that time. The solution was decanted off. The crystals were washed with *n*-pentane (3 x 3 mL) and dried under reduced pressure. [(Me₄TACD)Mg(μ-D)₂Mg(HMDS)₂] (1-d₂) (78 mg, 0.13 mmol) was obtained as slightly yellow crystals in 65% yield. ¹H NMR (THF-*d*₈; 400.1 MHz): δ 0.05 (s, 36H, N{Si(CH₃)₃}), 2.58 (s, 12H, CH₃-Me₄TACD), 2.65 - 2.72 (m, 8H, CH₂-Me₄TACD), 2.75 - 2.82 (m, 8H, CH₂-Me₄TACD) ppm. ²D NMR (THF; 400.1 MHz): δ 3.65 (MgD) ppm. ¹³C{¹H} NMR (THF-*d*₈; 100.6 MHz): δ 7.67 (N{Si(CH₃)₃}₂), 47.1 (CH₃-Me₄TACD), 56.4 (CH₂-Me₄TACD) ppm. ²⁹Si{¹H} NMR (THF-*d*₈; 79.5 MHz): δ -11.32 ppm.

¹H, ¹³C{¹H} and ²⁹Si{¹H} NMR spectra of [(Me₄TACD)Mg(μ-D)₂Mg(HMDS)₂] (1-d₂)

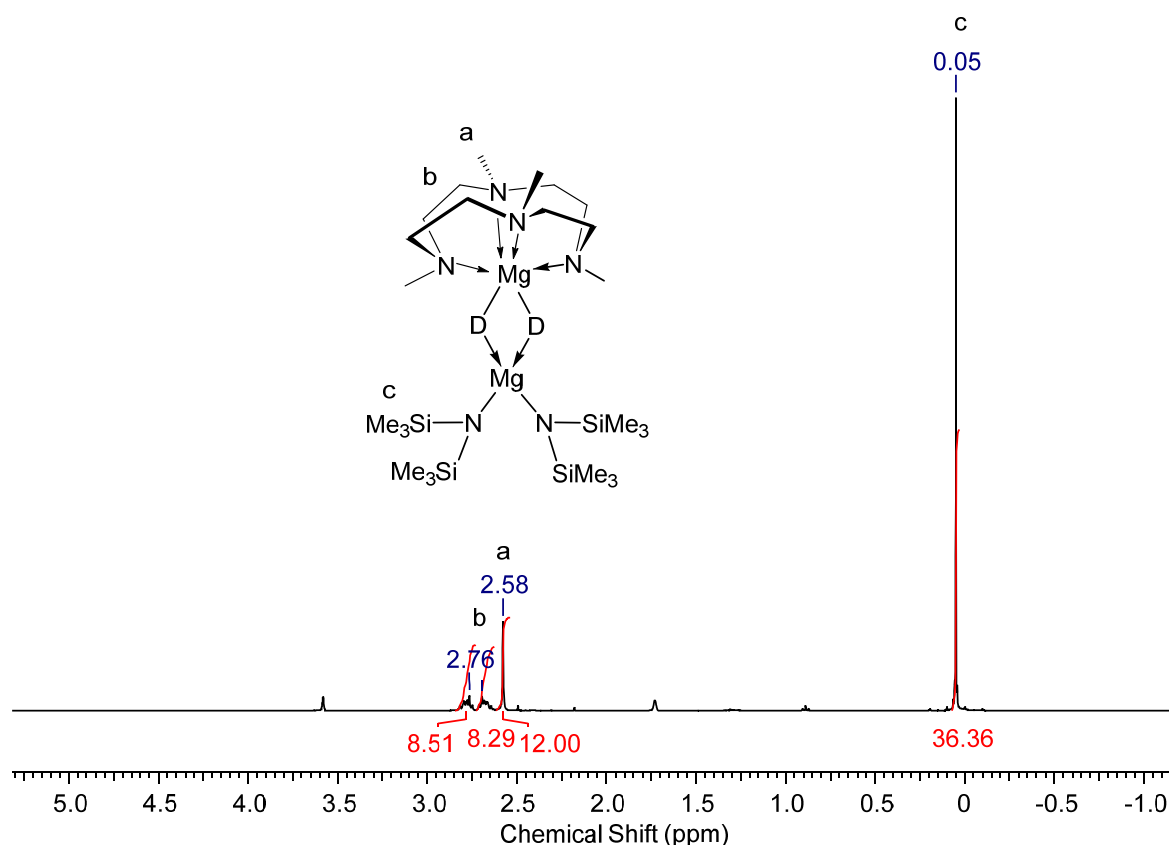


Figure S 4. ¹H NMR spectrum of 1-d₂ in THF-*d*₈ (*) at 25 °C.

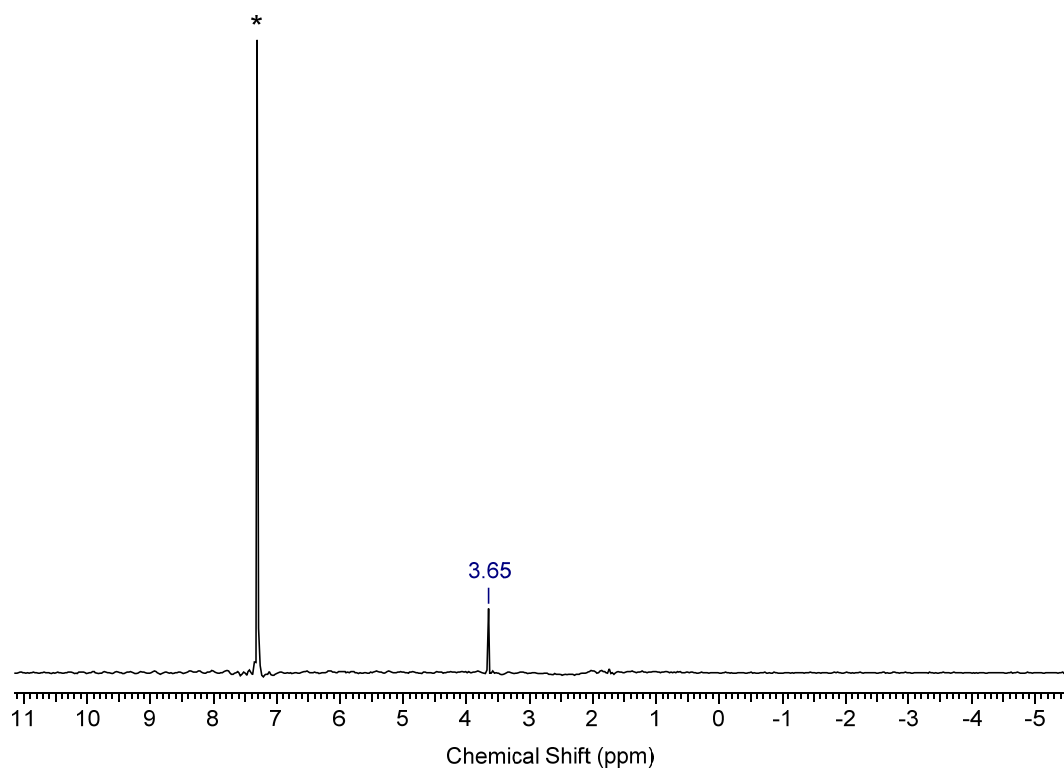


Figure S 5. ^2D NMR spectrum of $1\text{-}d_2$ in THF with benzene- d_6 as internal standard (*) at 25 °C.

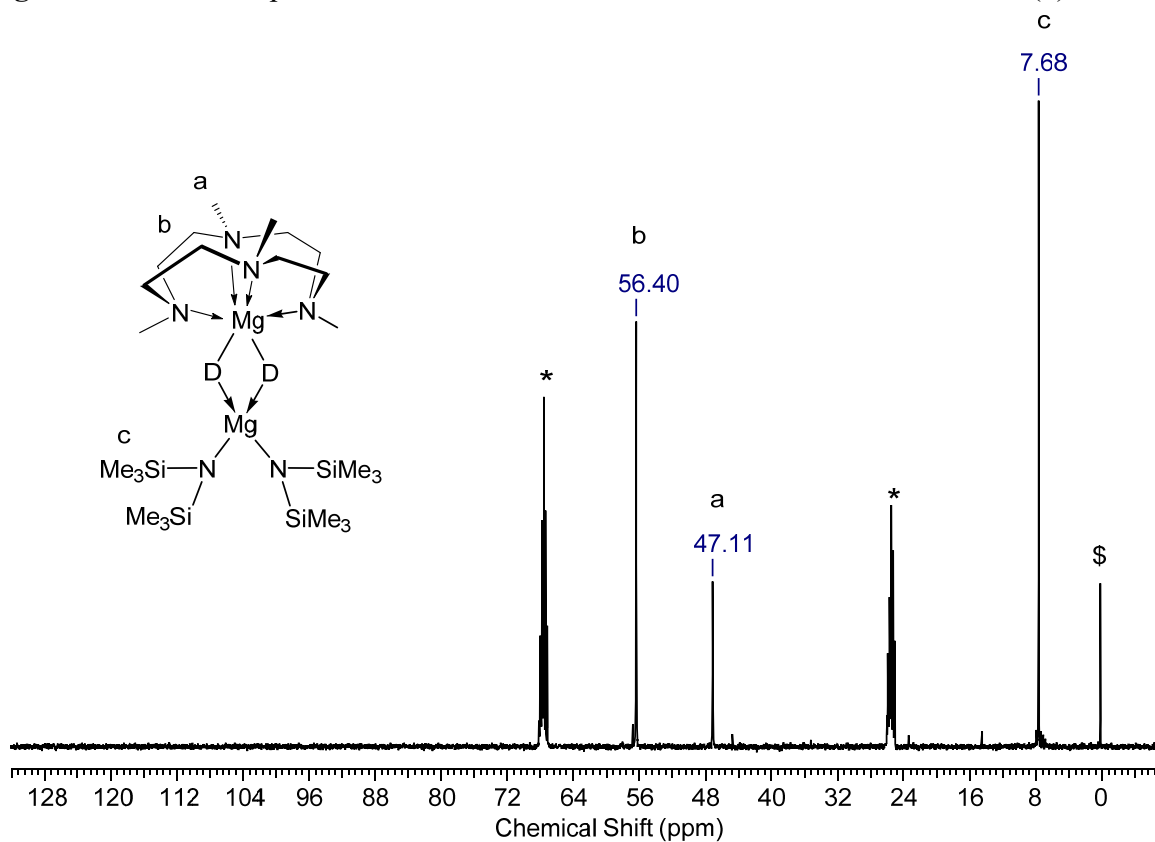


Figure S6. $^{13}\text{C}\{^1\text{H}\}$ NMR spectrum of $1\text{-}d_2$ in THF- d_8 (*) at 25 °C (\$ TMS).

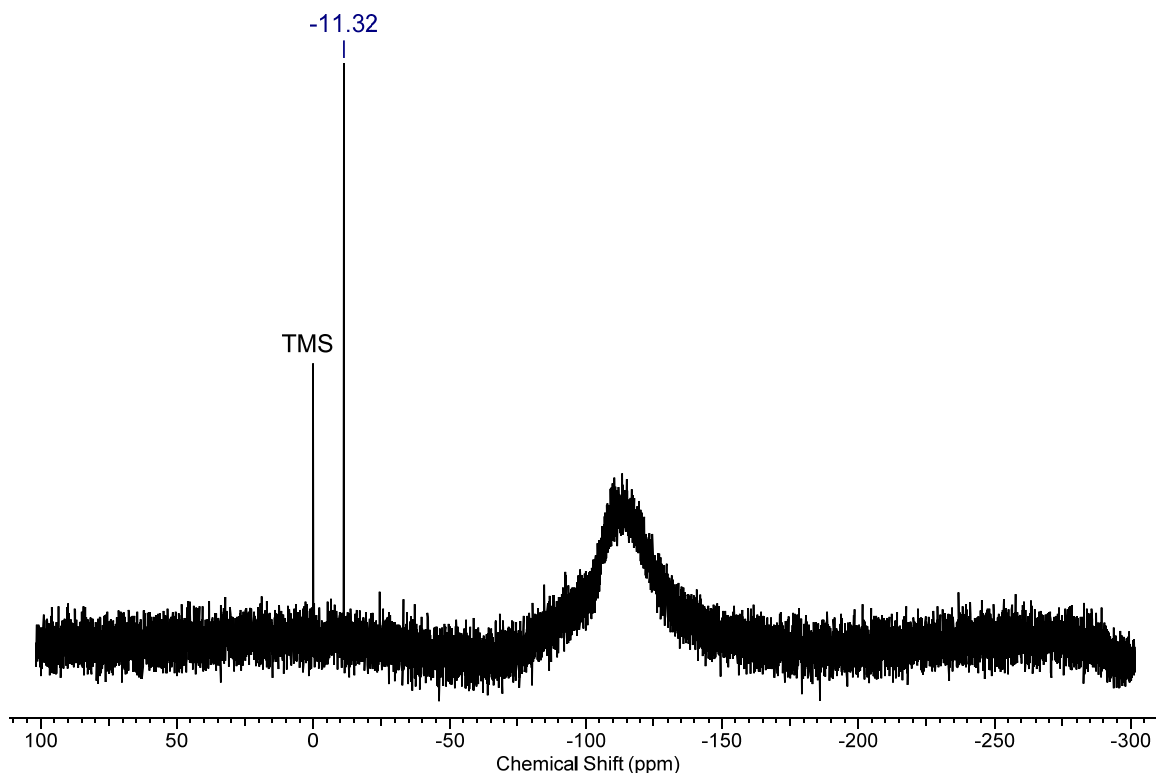


Figure S7. $^{29}\text{Si}\{^1\text{H}\}$ NMR spectrum of **1-d₂** in THF-*d*₈ at 25 °C.

[(Me₄TACD)₂Mg₂(μ-H)₂][B(3,5-Me₂-C₆H₃)₄]₂ (2). Solid [NEt₃H][B(3,5-Me₂-C₆H₃)₄] (213 mg, 0.4 mmol) was added in small portions to a solution of [(Me₄TACD)Mg(μ-H)₂Mg(HMDS)₂] (**1**) (240 mg, 0.4 mmol) in THF (6 mL) at room temperature. Gas evolution was observed. The reaction mixture was stirred for 30 min at room temperature and the solvent was removed under reduced pressure. The colorless solid was washed with toluene (5 x 3 mL) to remove the byproduct Mg(HMDS)₂. The solid residue was dried under vacuum to give [(Me₄TACD)₂Mg₂(μ-H)₂][B(3,5-Me₂-C₆H₃)₄]₂ (**2**) (232 mg, 0.17 mmol) in 43% yield. Single crystals suitable for X-ray analysis were obtained from a THF/*n*-hexane mixture at 25 °C over a period of 3 days. ^1H NMR (THF-*d*₈; 400.1 MHz): δ 2.10 (s, 48H, CH₃-B(3,5-Me₂-C₆H₃)₄), 2.24 - 2.33 (m, 16H, CH₂-Me₄TACD), 2.29 (s, 24H, CH₃-Me₄TACD), 2.37 - 2.45 (m, 16H, CH₂-Me₄TACD), 3.38 (s, 2H, MgH), 6.37 (m, 8H, *para*-CH-B(3,5-Me₂-C₆H₃)₄), 6.99 (m, 16H, *ortho*-CH-B(3,5-Me₂-C₆H₃)₄) ppm. $^{13}\text{C}\{^1\text{H}\}$ NMR (THF-*d*₈; 100.6 MHz): δ 22.5 (CH₃-B(3,5-Me₂-C₆H₃)₄), 44.0 (CH₃-Me₄TACD), 53.7 (CH₂-Me₄TACD), 123.8 (*para*-CH-B(3,5-Me₂-C₆H₃)₄), 133.1 (q, $^3J_{\text{BC}} = 2.9$ Hz, *meta*-C-B(3,5-Me₂-C₆H₃)₄), 135.7 (*ortho*-CH-B(3,5-Me₂-C₆H₃)₄), 165.9 (q, $^1J_{\text{BC}} = 49.2$ Hz, *ipso*-C-B(3,5-Me₂-C₆H₃)₄) ppm. $^{11}\text{B}\{^1\text{H}\}$ NMR (THF-*d*₈; 128.4 MHz): δ -8.88 ppm. Anal. calc. for C₈₈H₁₃₀N₈B₂Mg₂

(1370.29 g·mol⁻¹): C, 77.13; H, 9.56; N, 8.18; Mg, 3.55. Found: C, 76.89; H, 9.08; N, 7.65; Mg, 3.20%.

¹H, ¹³C{¹H} and ¹¹B{¹H} NMR spectra of [(Me₄TACD)₂Mg₂(μ-H)₂][B(3,5-Me₂-C₆H₃)₄]₂ (**2**)

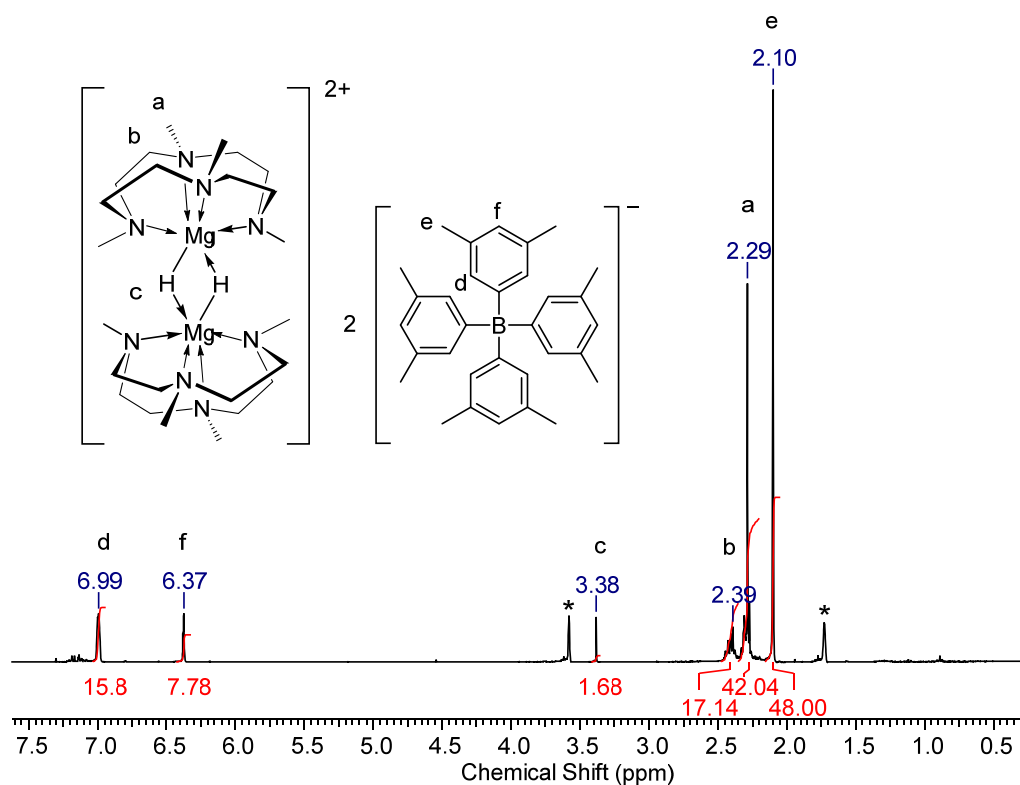
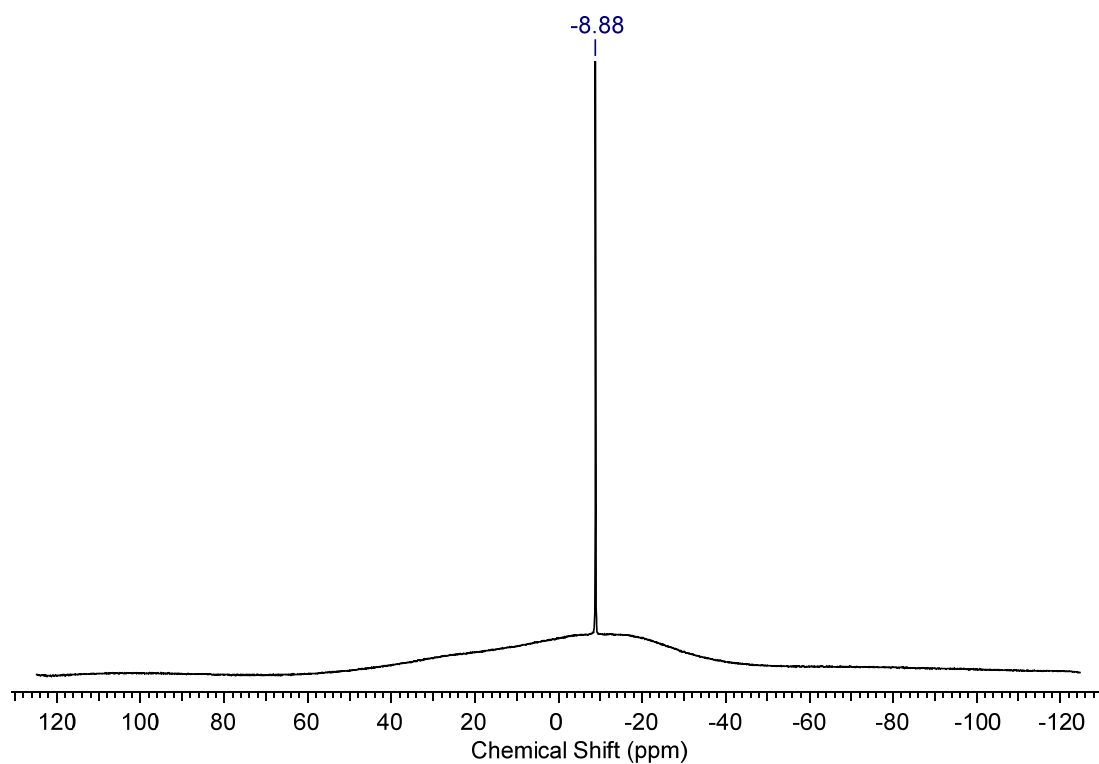
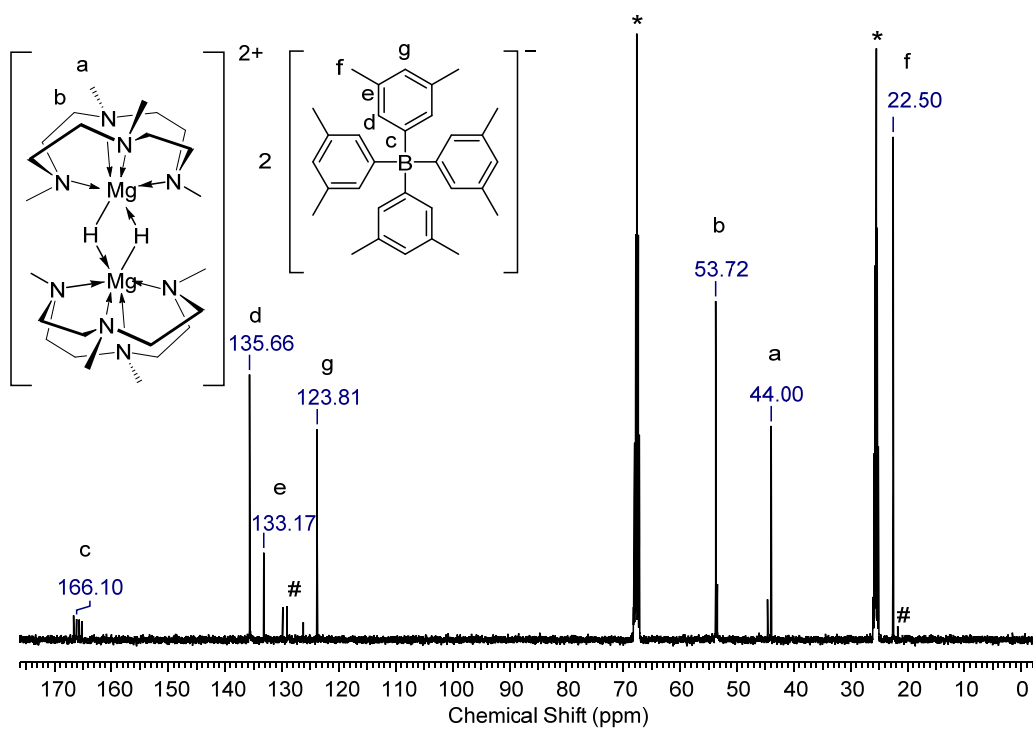


Figure S8. ¹H NMR spectrum of **2** in THF-*d*₈ (*) at 25 °C.



[(Me₄TACD)₂Mg₂(μ-D)]₂[B(3,5-Me₂-C₆H₃)₄]₂ (**2-d₂**). A suspension of [NEt₃H][B(3,5-Me₂-C₆H₃)₄] (47 mg, 0.09 mmol) in THF (2mL) was added slowly to a solution of [(Me₄TACD)Mg(μ-D)₂Mg(HMDS)₂] (**1-d₂**) (55 mg, 0.09 mmol) at room temperature. Gas evolution was observed. The reaction mixture was stirred for 30 min at room temperature and the solvent was removed under reduced pressure. The colorless solid was washed with toluene (5 x 3 mL) to remove the byproduct Mg(HMDS)₂. The solid residue was dried under vacuum to give [(Me₄TACD)₂Mg₂(μ-H)]₂[B(3,5-Me₂-C₆H₃)₄]₂ (**2-d₂**) (49 mg, 0.04 mmol) in 79% yield. ¹H NMR (THF-*d*₈; 400.1 MHz): δ 2.10 (s, 24H, CH₃-B(3,5-Me₂-C₆H₃)₄), 2.24 - 2.30 (m, 8H, CH₂-Me₄TACD), 2.27 (s, 12H, CH₃-Me₄TACD), 2.36 - 2.43 (m, 8H, CH₂-Me₄TACD), 6.38 (m, 4H, *para*-CH-B(3,5-Me₂-C₆H₃)₄), 7.00 (m, 8H, *ortho*-CH-B(3,5-Me₂-C₆H₃)₄) ppm. ²D NMR (THF; 400.1 MHz): δ 3.44 (MgD) ppm. ¹³C{¹H} NMR (THF-*d*₈; 100.6 MHz): δ 22.5 (CH₃-B(3,5-Me₂-C₆H₃)₄), 44.1 (CH₃-Me₄TACD), 53.8 (CH₂-Me₄TACD), 123.8 (*para*-CH-B(3,5-Me₂-C₆H₃)₄), 133.2 (q, ³J_{BC} = 2.9 Hz, *meta*-C-B(3,5-Me₂-C₆H₃)₄), 135.7 (*ortho*-CH-B(3,5-Me₂-C₆H₃)₄), 165.9 (q, ¹J_{BC} = 49.2 Hz, *ipso*-C-B(3,5-Me₂-C₆H₃)₄) ppm. ¹¹B{¹H} NMR (THF-*d*₈; 128.4 MHz): δ -7.00 ppm.

¹H, ¹³C{¹H} and ¹¹B{¹H} NMR spectra of [(Me₄TACD)₂Mg₂(μ-D)]₂[B(3,5-Me₂-C₆H₃)₄]₂ (**2-d₂**)

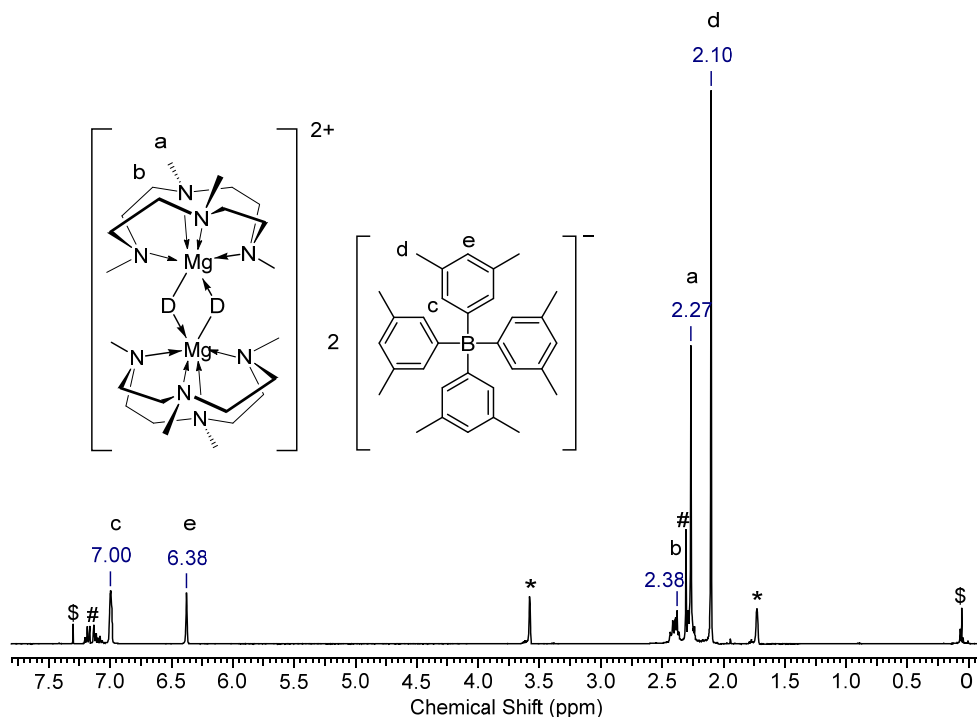


Figure S11. ¹H NMR spectrum of **2-d₂** in THF-*d*₈ (*) at 25 °C (# toluene, \$ Mg(HMDS)₂).

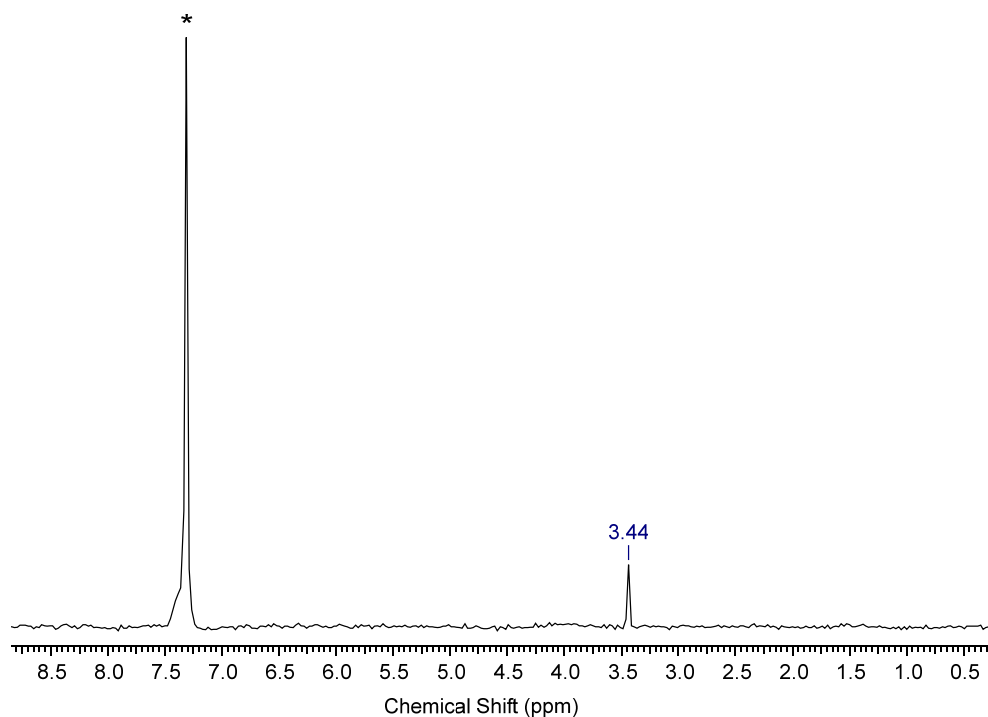


Figure S12. ^2D NMR spectrum of $2\text{-}d_2$ in THF with benzene- d_6 (*) as internal standard at 25 °C.

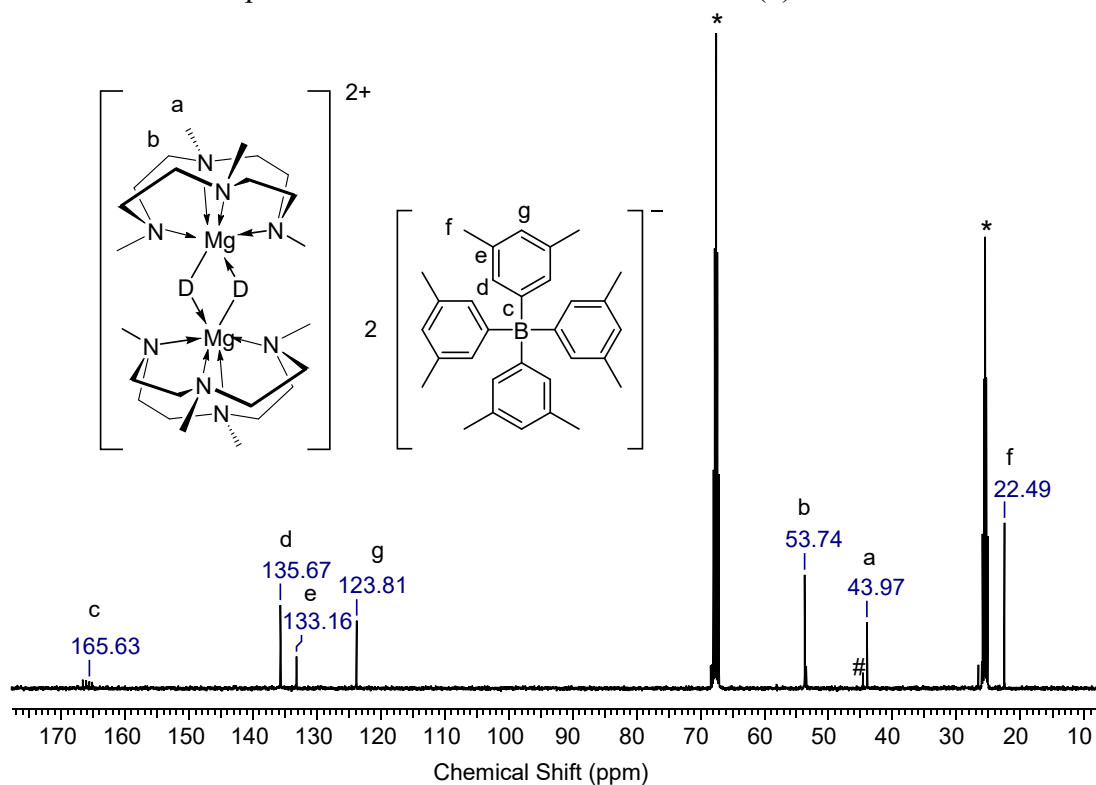


Figure S13. $^{13}\text{C}\{^1\text{H}\}$ NMR spectrum of $2\text{-}d_2$ in THF- d_8 (*) at 25 °C (# unidentified species).

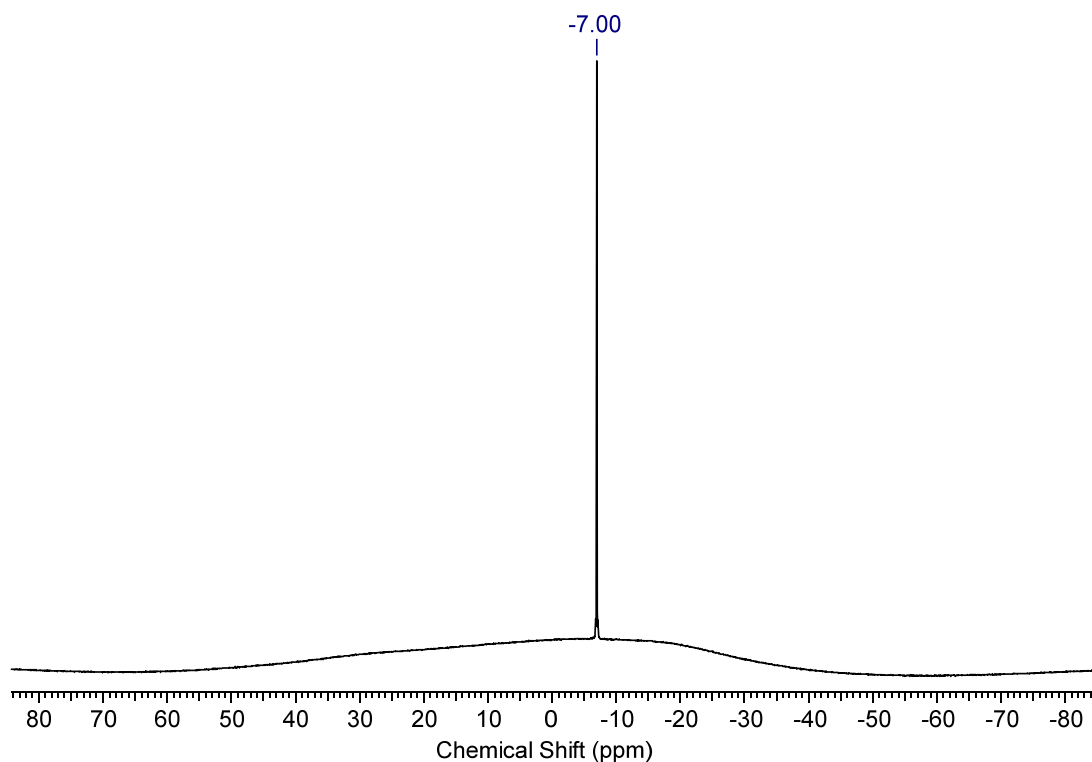


Figure S14. $^{11}\text{B}\{^1\text{H}\}$ NMR spectrum of **2-d₂** in THF-*d*₈ at 25 °C.

[(Me₄TACD)Mg(μ-H)₃BH][B(3,5-Me₂-C₆H₃)₄] (3). A solution of BH₃·THF (1 M in THF, 0.1 mL, 0.1 mmol) was added to a solution of [(Me₄TACD)₂Mg₂(μ-H)₂][B(3,5-Me₂-C₆H₃)₄]₂ (68 mg, 0.05 mmol) in THF (2mL) at room temperature and the reaction mixture was stirred for 30 min. The solvent was removed under reduced pressure and the colorless solid was washed with *n*-pentane (3 mL). The solid residue was dried under vacuum to give [(Me₄TACD)Mg(μ-H)₃BH][B(3,5-Me₂-C₆H₃)₄] (**3**) (59 mg, 0.08 mmol) in 84% yield. Single crystals suitable for X-ray analysis were obtained from a THP/cyclohexane mixture at 25 °C over a period of 16 h. ^1H NMR (THF-*d*₈; 400.1 MHz): δ -0.46 (quart, $^1J_{\text{BH}} = 82.0$ Hz, 4H, BH₄), 2.10 (s, 24H, CH₃-B(3,5-Me₂-C₆H₃)₄), 2.29 - 3.35 (m, 8H, CH₂-Me₄TACD), 2.31 (s, 12H, CH₃-Me₄TACD), 2.39 - 2.45 (m, 8H, CH₂-Me₄TACD), 6.38 (m, 4H, *para*-CH-B(3,5-Me₂-C₆H₃)₄), 7.00 (m, 8H, *ortho*-CH-B(3,5-Me₂-C₆H₃)₄) ppm. $^{13}\text{C}\{^1\text{H}\}$ NMR (THF-*d*₈; 100.6 MHz): δ 22.5 (CH₃-B(3,5-Me₂-C₆H₃)₄), 44.7 (CH₃-Me₄TACD), 53.5 (CH₂-Me₄TACD), 123.9 (*para*-CH-B(3,5-Me₂-C₆H₃)₄), 133.3 (q, $^3J_{\text{BC}} = 2.9$ Hz, *meta*-C-B(3,5-Me₂-C₆H₃)₄), 135.7 (*ortho*-CH-B(3,5-Me₂-C₆H₃)₄), 165.9 (q, $^1J_{\text{BC}} = 49.2$ Hz, *ipso*-C-B(3,5-Me₂-C₆H₃)₄) ppm. ^{11}B NMR (THF-*d*₈; 128.4 MHz): δ -7.00 (B(3,5-Me₂-C₆H₃)₄), -44.9, (quint, $^1J_{\text{BH}} = 82.0$ Hz, BH₄) ppm. IR (KBr): ν = 3024 (w), 3004 (s), 2972 (m), 2913 (s),

2871 (m), 2444 (w), 2291 (w), 2214 (w), 1575 (m), 1470 (s), 1358 (w), 1298 (m), 1268 (w), 1249 (w), 1148 (m), 1108 (w), 1078 (m), 1050 (w), 1022 (m), 967 (m), 906 (w), 842 (m), 800 (w), 756 (w), 734 (m), 584 (w), 505 (w), 473(w) cm^{-1} . Anal. calc. for $\text{C}_{44}\text{H}_{68}\text{N}_4\text{B}_2\text{Mg}$ ($698.98 \text{ g}\cdot\text{mol}^{-1}$): C, 75.61; H, 9.81; N, 8.02; Mg, 3.48. Found: C, 73.40; H, 9.33; N, 7.77; Mg, 3.47%.

^1H , $^{13}\text{C}\{^1\text{H}\}$ and ^{11}B NMR spectra of $[(\text{Me}_4\text{TACD})\text{Mg}(\mu\text{-H})_3\text{BH}][\text{B}(\text{3,5-Me}_2\text{-C}_6\text{H}_3)_4]$ (3**)**

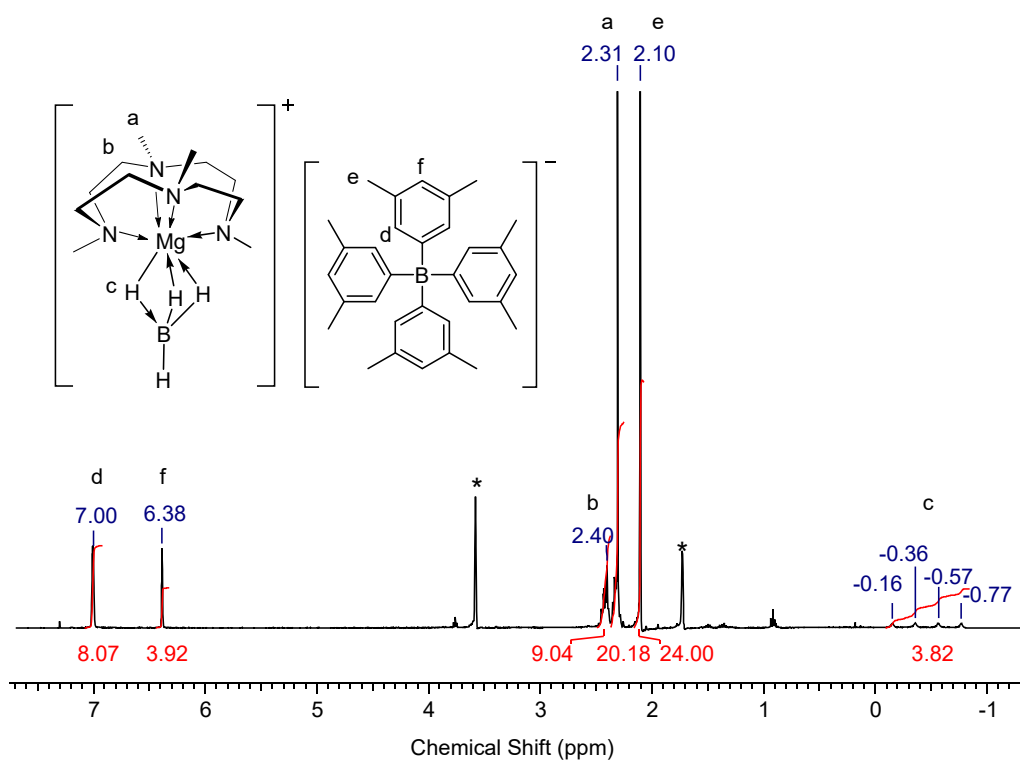


Figure S15. ^1H NMR spectrum of **3** in $\text{THF-}d_8$ (*) at $25 \text{ }^\circ\text{C}$.

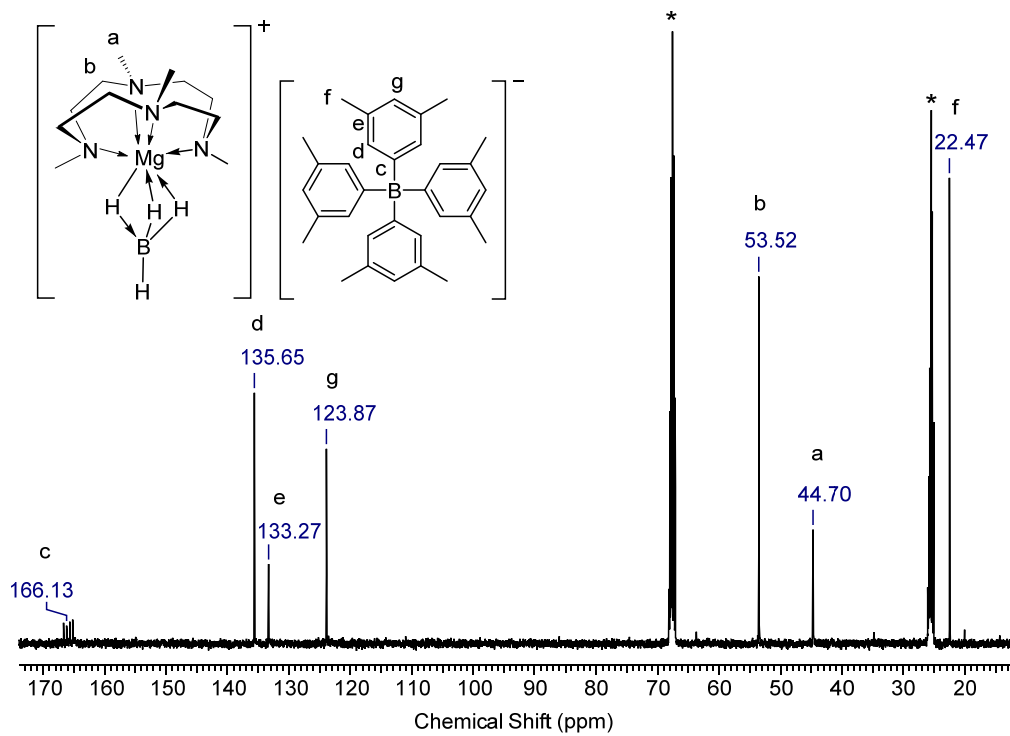


Figure S16. $^{13}\text{C}\{^1\text{H}\}$ NMR spectrum of **3** in $\text{THF-}d_8$ (*) at $25\text{ }^\circ\text{C}$.

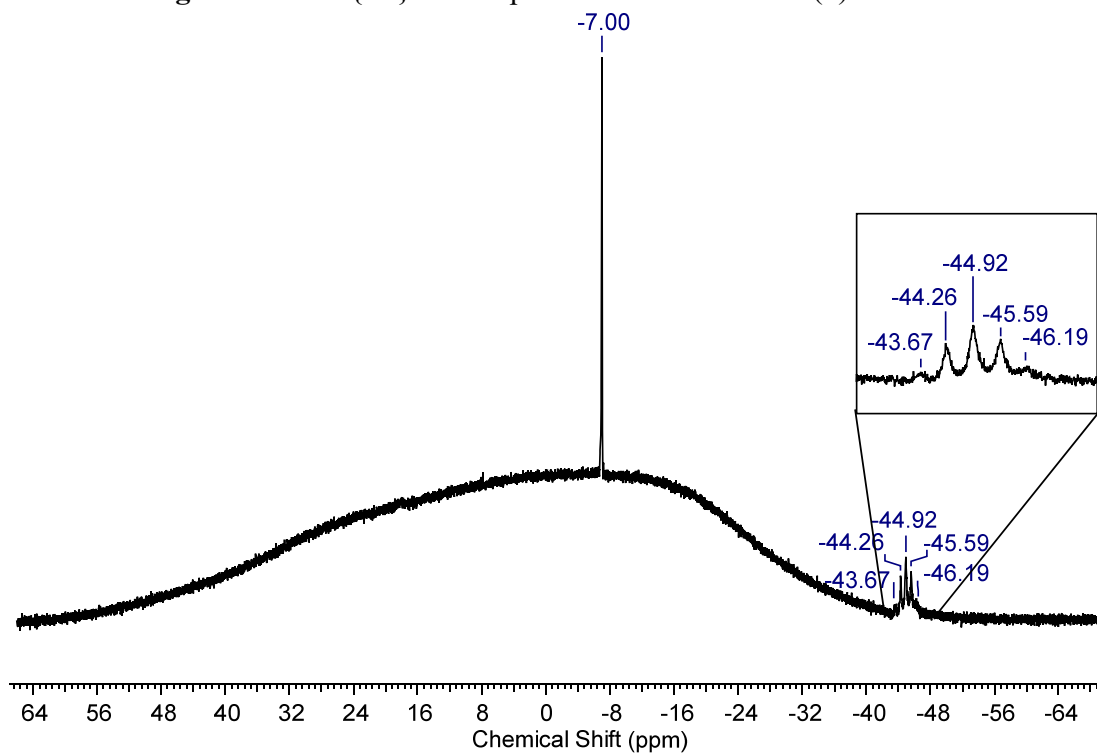


Figure S17. ^{11}B NMR spectrum of **3** in $\text{THF-}d_8$ at $25\text{ }^\circ\text{C}$.

[(Me₄TACD)Mg(μ-H)BHpin)][B(3,5-Me₂-C₆H₃)₄] (4). A solution of pinacolborane (22 μL, 19 mg, 0.15 mmol) in THF (1 mL) was added to a solution of [(Me₄TACD)₂Mg₂(μ-H)₂][B(3,5-Me₂-C₆H₃)₄]₂ (**2**) (103 mg, 0.075 mmol) in THF (3 mL) and the reaction solution was stirred for 15 min at 25 °C. The solvent was removed under reduced pressure and the colorless solid was washed with *n*-pentane (3 mL) and dried under vacuum. [(Me₄TACD)Mg(μ-H)BHpin)][B(3,5-Me₂-C₆H₃)₄] (**4**) (115 mg, 0.14 mmol) was obtained in 94% yield. ¹H NMR (THF-*d*₈; 400.1 MHz): δ 1.13 (s, 12H, CH₃-BPin), 2.10 (s, 24H, CH₃-[B(3,5-Me₂-C₆H₃)₄]), 2.32 - 2.43 (m, 16H, CH₂-Me₄TACD), 2.39 (s, 12H, CH₃-Me₄TACD), 6.38 (m, 4H, *para*-CH-[B(3,5-Me₂-C₆H₃)₄]), 7.00 (m, 8H, *ortho*-CH-[B(3,5-Me₂-C₆H₃)₄]) ppm, BH resonance not detected. ¹³C{¹H} NMR (THF-*d*₈; 100.6 MHz): δ 22.5 (CH₃-[B(3,5-Me₂-C₆H₃)₄]), 25.3 (s, 12H, CH₃-BPin, identified by HSQC NMR), 45.7 (CH₃-Me₄TACD), 54.6 (CH₂-Me₄TACD), 123.9 (*para*-CH-[B(3,5-Me₂-C₆H₃)₄]), 133.2 (q, ³J_{BC} = 2.9 Hz, *meta*-C-[B(3,5-Me₂-C₆H₃)₄]), 135.7 (*ortho*-CH-[B(3,5-Me₂-C₆H₃)₄]), 165.9 (q, ¹J_{BC} = 49.2 Hz, *ipso*-C-[B(3,5-Me₂-C₆H₃)₄]) ppm. ¹¹B NMR (THF-*d*₈; 128.4 MHz): δ 1.42 (br, BPin), -8.88 (B(3,5-Me₂-C₆H₃)₄) ppm. IR (KBr): ν = 3024 (w), 3000 (s), 2973 (s), 2913 (s), 2866 (m), 2282 (w), 2197 (w), 1575 (m), 1501 (m), 1467 (s), 1384 (w), 1359 (w), 1298 (m), 1269 (w), 1249 (w), 1213 (w), 1156 (s), 1109 (w), 1080 (m), 1049 (w), 1025 (m), 967 (m), 906 (w), 840 (m), 800 (w), 756 (w), 736 (m), 691 (w), 662 (w), 581 (w), 507 (w), 448(w) cm⁻¹. Anal. calc. for C₅₀H₇₈N₄O₂Mg (813.13 g·mol⁻¹): C, 73.86; H, 9.67; N, 6.89; Mg, 2.99. Found: C, 72.01; H, 9.25; N, 6.67; Mg, 2.58 %.

^1H , $^{13}\text{C}\{^1\text{H}\}$ -APT, and $^{11}\text{B}\{^1\text{H}\}$ NMR spectra of $[(\text{Me}_4\text{TACD})\text{Mg}(\mu\text{-H})\text{BHpin}][\text{B}(3,5\text{-Me}_2\text{-C}_6\text{H}_3)_4]$ (**4**).

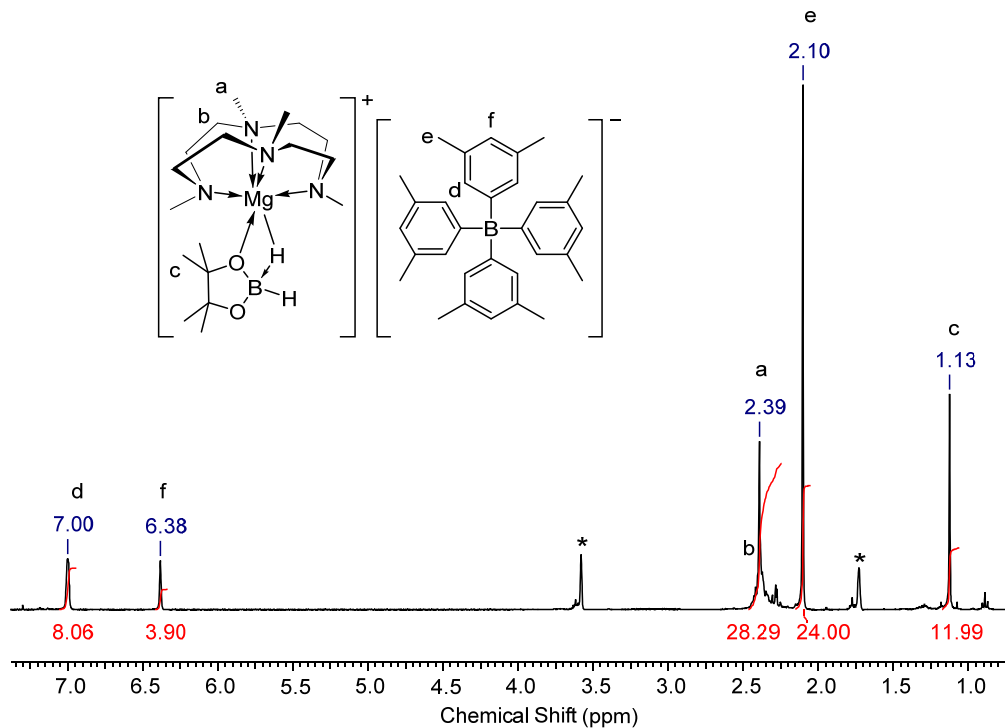


Figure S18. ^1H NMR spectrum of **4** in $\text{THF-}d_8$ (*) at $25\text{ }^\circ\text{C}$.

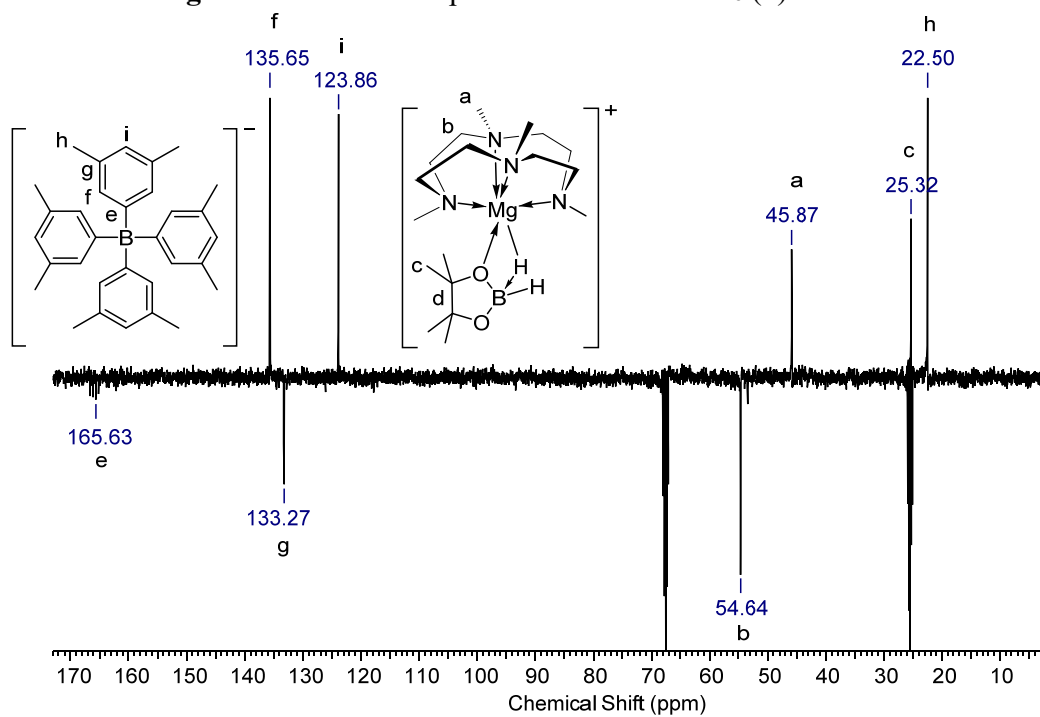


Figure S19. $^{13}\text{C}\{^1\text{H}\}$ -APT NMR spectrum of **4** in $\text{THF-}d_8$ (*) at $25\text{ }^\circ\text{C}$.

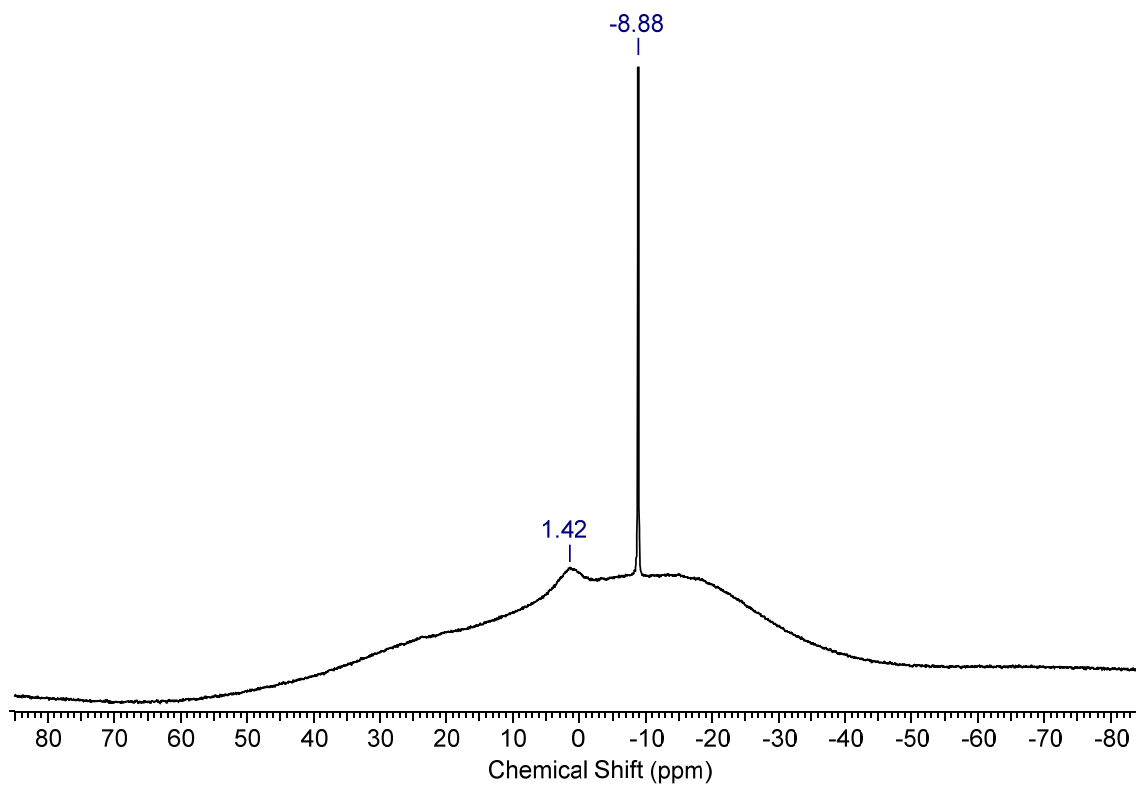


Figure S20. ^{11}B NMR spectrum of **4** in $\text{THF-}d_8$ at 25 °C.

Solid state structure of $[(\text{Me}_4\text{TACD})\text{Mg}(\mu\text{-H})\text{BHPin}][\text{B}(3,5\text{-Me}_2\text{-C}_6\text{H}_3)_4]$ (4**)**

Single crystals of $[(\text{Me}_4\text{TACD})\text{Mg}(\mu\text{-H})\text{BHPin}][\text{B}(3,5\text{-Me}_2\text{-C}_6\text{H}_3)_4]$ (**4**) were obtained from a THF/cyclohexane mixture at -30 °C over a period of 16 h. **4** displays a monomeric structure with a magnesium centre coordinated by four nitrogen atoms of the Me_4TACD ligand and by one hydride and one oxygen atom of the pinacolborate ligand (Figure S21).

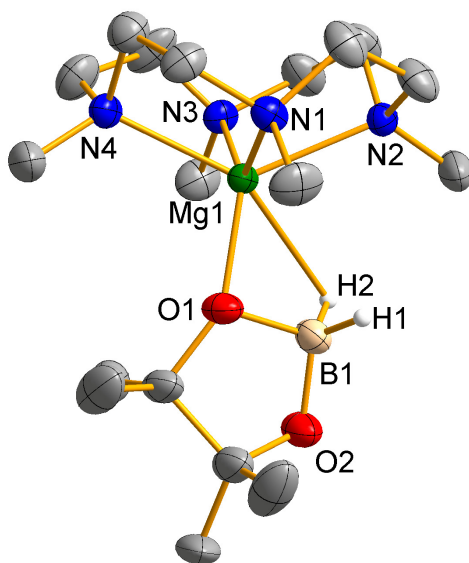


Figure S21. Molecular structure of $[(\text{Me}_4\text{TACD})\text{Mg}(\mu\text{-H})\text{BHPin}][\text{B}(3,5\text{-Me}_2\text{-C}_6\text{H}_3)_4]$ (**4**). Displacement parameters are shown at the 50% probability level. Hydrogen atoms, except for the hydrides H1 and H2, are omitted for clarity. The borate anion is not shown. Selected interatomic distances [\AA] and angles [$^\circ$]: $\text{Mg1}\cdots\text{B1}$ 2.593(4), $\text{Mg1}\cdots\text{H1}$ 2.75(5), $\text{Mg1}\text{-H2}$ 2.56(4), $\text{Mg1}\text{-N1}$ 2.217(3), $\text{Mg1}\text{-N2}$ 2.287(3), $\text{Mg1}\text{-N3}$ 2.222(3), $\text{Mg1}\text{-N4}$ 2.280(3).

$[(\text{Me}_4\text{TACD})\text{Mg}(\text{H}_2\text{Al}^i\text{Bu}_2)][\text{B}(3,5\text{-Me}_2\text{-C}_6\text{H}_3)_4]$ (**5**). Neat DIBAL(H) (14 mg, 0.1 mmol) was added to a solution of $[(\text{Me}_4\text{TACD})_2\text{Mg}_2(\mu\text{-H})_2][\text{B}(3,5\text{-Me}_2\text{-C}_6\text{H}_3)_4]_2$ (68 mg, 0.05 mmol) in THF (2mL) at room temperature and the reaction mixture was stirred for 30 min. The solvent was removed under reduced pressure and the colorless solid was washed with *n*-pentane (3 mL). The solid residue was dried under vacuum to give $[(\text{Me}_4\text{TACD})\text{Mg}(\text{H}_2\text{Al}^i\text{Bu}_2)][\text{B}(3,5\text{-Me}_2\text{-C}_6\text{H}_3)_4]$ (**5**) (69 mg, 0.08 mmol) in 83% yield. ^1H NMR (THF-*d*₈; 400.1 MHz): δ 0.02 (d, $^3J_{\text{HH}} = 7.0$ Hz, 4H, $\text{CH}_2\text{-Al}^i\text{Bu}_2$), 0.95 (d, $^3J_{\text{HH}} = 6.5$ Hz, 12H, $\text{CH}_3\text{-Al}^i\text{Bu}_2$), 1.81 (sept, $^3J_{\text{HH}} = 6.8$ Hz, 2H, $\text{CH-Al}^i\text{Bu}_2$), 2.10 (s, 24H, $\text{CH}_3\text{-B}(3,5\text{-Me}_2\text{-C}_6\text{H}_3)_4$), 2.29 (s, 12H, $\text{CH}_3\text{-Me}_4\text{TACD}$), 2.29 - 2.35 (m, 8H, $\text{CH}_2\text{-Me}_4\text{TACD}$), 2.39 - 2.46 (m, 8H, $\text{CH}_2\text{-Me}_4\text{TACD}$), 3.04 (br s, 2H, MgH_2Al), 6.39 (m, 4H, *para*- $\text{CH-B}(3,5\text{-Me}_2\text{-C}_6\text{H}_3)_4$), 7.00 (m, 8H, *ortho*- $\text{CH-B}(3,5\text{-Me}_2\text{-C}_6\text{H}_3)_4$) ppm. $^{13}\text{C}\{^1\text{H}\}$ NMR (THF-*d*₈; 100.6 MHz): δ 19.9 ($\text{CH}_2\text{-Al}^i\text{Bu}_2$), 22.5 ($\text{CH}_3\text{-B}(3,5\text{-Me}_2\text{-C}_6\text{H}_3)_4$), 28.2 ($\text{CH-Al}^i\text{Bu}_2$), 28.6 ($\text{CH}_3\text{-Al}^i\text{Bu}_2$), 44.8 ($\text{CH}_3\text{-Me}_4\text{TACD}$), 53.6 ($\text{CH}_2\text{-Me}_4\text{TACD}$), 123.9 (*para*- $\text{CH-B}(3,5\text{-Me}_2\text{-C}_6\text{H}_3)_4$), 133.3 (q, $^3J_{\text{BC}} = 2.9$ Hz, *meta*- $\text{C-B}(3,5\text{-Me}_2\text{-C}_6\text{H}_3)_4$), 135.7 (*ortho*- $\text{CH-B}(3,5\text{-Me}_2\text{-C}_6\text{H}_3)_4$), 165.9 (q, $^1J_{\text{BC}} = 49.2$ Hz, *ipso*- $\text{C-B}(3,5\text{-Me}_2\text{-C}_6\text{H}_3)_4$) ppm. ^{27}Al NMR (THF-*d*₈; 104.3 MHz): δ 130.8 ppm. $^{11}\text{B}\{^1\text{H}\}$ NMR (THF-*d*₈; 128.4 MHz): δ -7.00 ppm. IR (KBr): $\nu = 3745$ (w), 3025 (w), 3003 (m), 2974 (s), 2917 (s), 2857 (m), 1654 (w), 1576 (m), 1541 (m), 1465 (s), 1357 (w), 1298 (m),

1242 (s), 1149 (s), 1078 (w), 1061 (w), 1021 (w), 966 (w), 904 (w), 841 (m), 792 (m), 754 (w), 736 (m), 664 (w), 581 (w), 507 (w) cm^{-1} . Anal. calc. for $\text{C}_{52}\text{H}_{84}\text{N}_4\text{BMg}$ ($827.37 \text{ g}\cdot\text{mol}^{-1}$): C, 75.49; H, 10.23; N, 6.77; Mg, 2.94; Al 3.26. Found: C, 74.17; H, 9.95; N, 6.96; Mg, 3.29; Al, 3.04%.

^1H , $^{13}\text{C}\{^1\text{H}\}$, ^{27}Al and $^{11}\text{B}\{^1\text{H}\}$ NMR spectra of $[(\text{Me}_4\text{TACD})\text{Mg}(\text{H}_2\text{Al}^i\text{Bu}_2)][\text{B}(3,5\text{-Me}_2\text{-C}_6\text{H}_3)_4]$ (**5**)

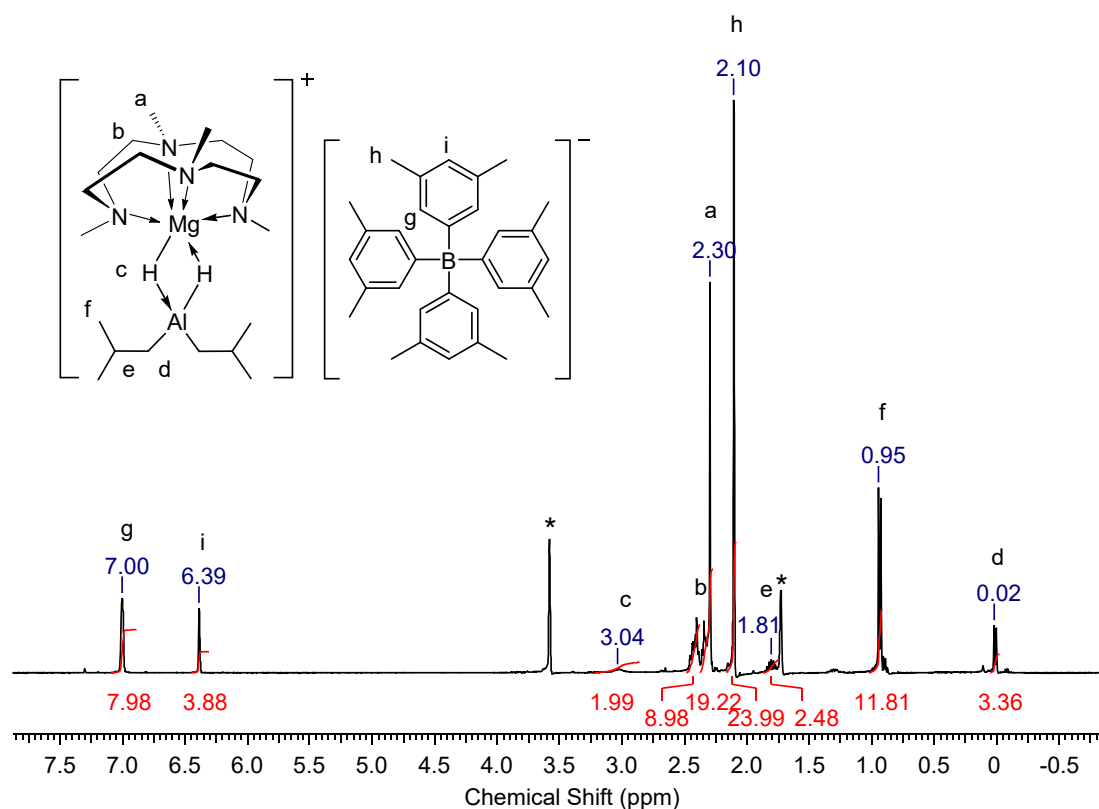


Figure S22. ^1H NMR spectrum of **5** in $\text{THF-}d_8$ (*) at $25 \text{ }^\circ\text{C}$.

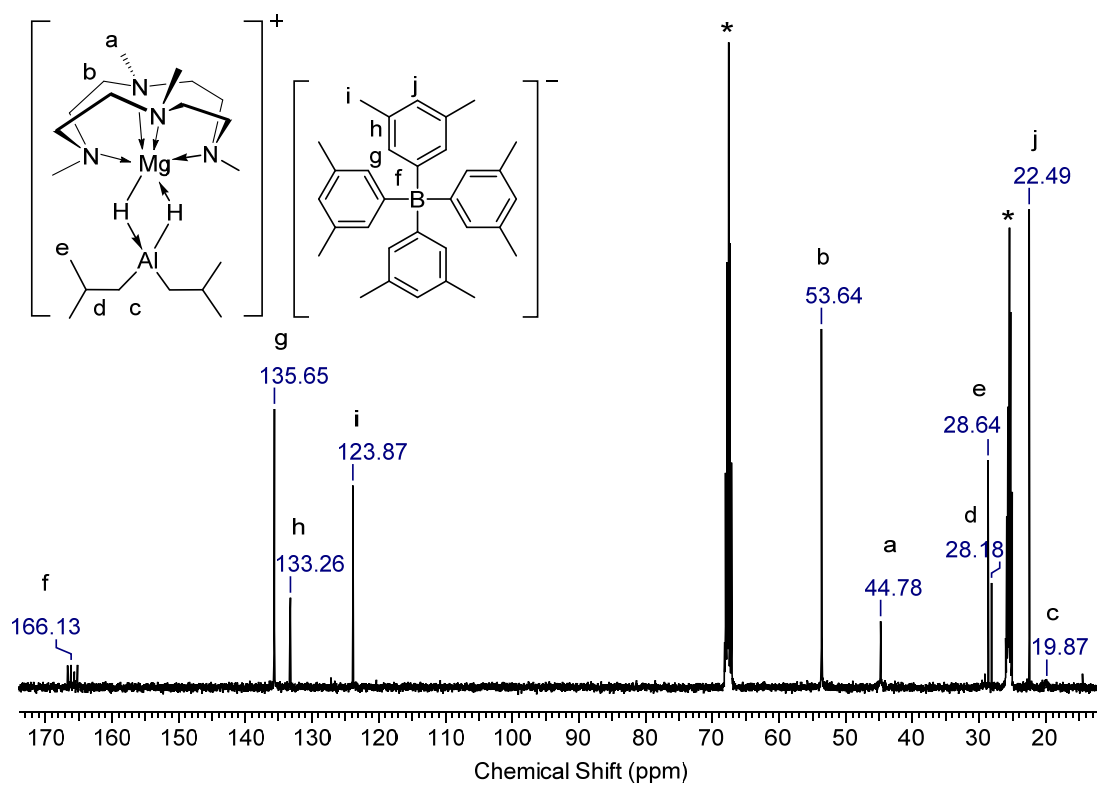


Figure S23. $^{13}\text{C}\{^1\text{H}\}$ NMR spectrum of **5** in $\text{THF-}d_8$ (*) at 25 °C.

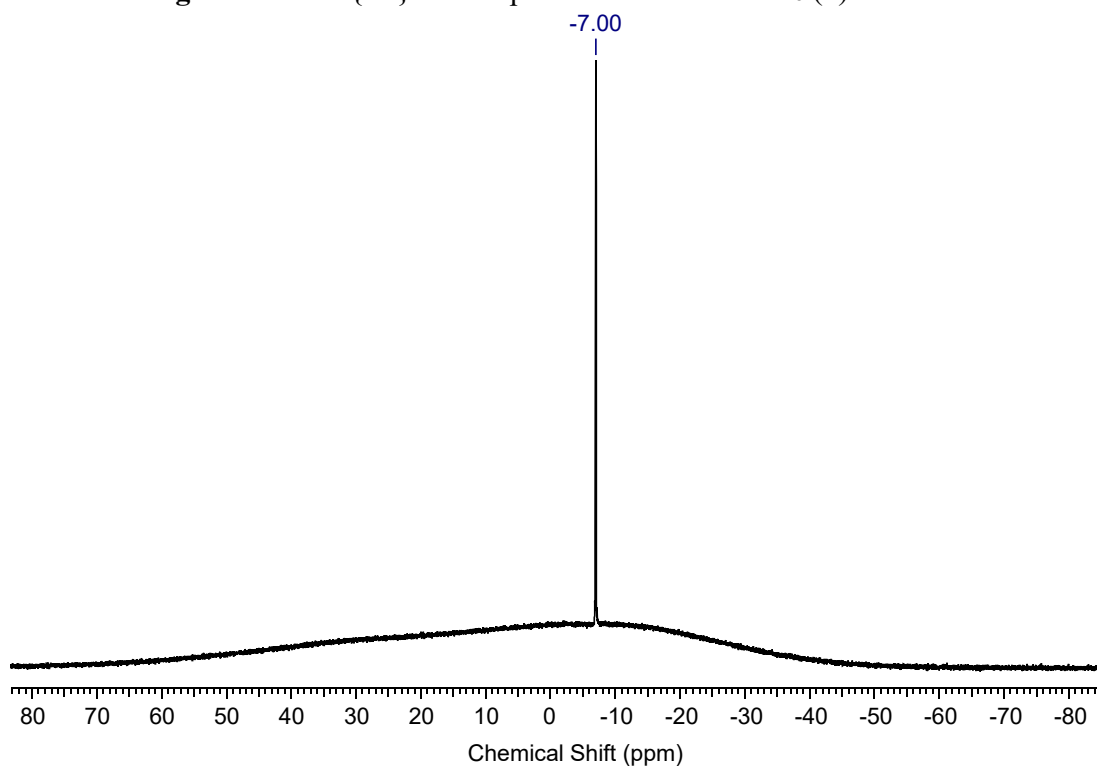


Figure S24. $^{11}\text{B}\{^1\text{H}\}$ NMR spectrum of **5** in $\text{THF-}d_8$ at 25 °C.

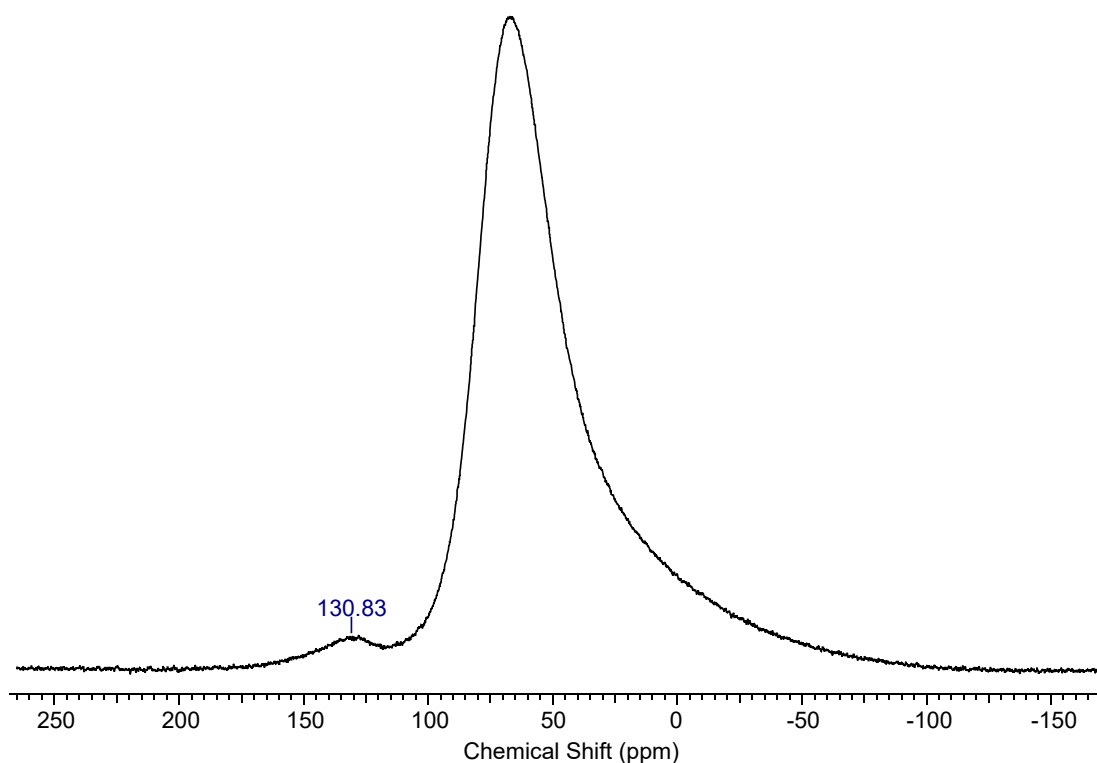


Figure S25. ^{27}Al NMR spectrum of **5** in $\text{THF-}d_8$ at $25\text{ }^\circ\text{C}$.

$[(\text{Me}_4\text{TACD})\text{Mg}(\text{OCH}_2\text{Ph})][\text{B}(3,5\text{-Me}_2\text{-C}_6\text{H}_3)_4]$ (6**).** To a solution of $[(\text{Me}_4\text{TACD})_2\text{Mg}_2(\mu\text{-H})_2][\text{B}(3,5\text{-Me}_2\text{-C}_6\text{H}_3)_4]_2$ (**2**) (68 mg, 0.05 mmol) in THF (4 mL) a solution of benzaldehyde (11 mg, 0.1 mmol) in THF (1 mL) was added and the reaction mixture was stirred for 10 min at room temperature. The solvent was removed under reduced pressure and the colorless solid residue was washed with diethyl ether (6 mL) and *n*-pentane (4.5 mL). The solid was dried under vacuum to give $[(\text{Me}_4\text{TACD})\text{Mg}(\text{OCH}_2\text{Ph})][\text{B}(3,5\text{-Me}_2\text{-C}_6\text{H}_3)_4]$ (**7**) (74 mg, 0.08 mmol) in 85% yield. Single crystals suitable for X-ray analysis were obtained from THF/*n*-pentane over a period of 16 h at $25\text{ }^\circ\text{C}$. ^1H NMR ($\text{THF-}d_8$; 400.1 MHz): δ 2.09 (s, 24H, $\text{CH}_3\text{-B}(3,5\text{-Me}_2\text{-C}_6\text{H}_3)_4$), 2.30 - 2.44 (m, 16H, $\text{CH}_2\text{-Me}_4\text{TACD}$), 2.32 (s, 12H, $\text{CH}_3\text{-Me}_4\text{TACD}$), 4.92 (s, 2H, OCH_2Ph), 6.37 (m, 4H, *para-CH-B*(3,5-Me₂-C₆H₃)₄), 7.00 (m, 8H, *ortho-CH-B*(3,5-Me₂-C₆H₃)₄), 7.04 (m, 1H, *para-CH-OCH*₂Ph), 7.17 (m, 2H, *meta-CH-OCH*₂Ph), 7.27 (m, 2H, *ortho-CH-OCH*₂Ph) ppm. $^{13}\text{C}\{^1\text{H}\}$ NMR ($\text{THF-}d_8$; 100.6 MHz): δ 22.5 ($\text{CH}_3\text{-[B}(3,5\text{-Me}_2\text{-C}_6\text{H}_3)_4]$), 45.7 ($\text{CH}_3\text{-Me}_4\text{TACD}$), 54.4 ($\text{CH}_2\text{-Me}_4\text{TACD}$), 68.4 (OCH_2Ph), 123.8 (*para-CH-B*(3,5-Me₂-C₆H₃)₄), 126.1 (*para-CH-OCH*₂Ph), 126.7 (*meta-CH-OCH*₂Ph), 128.4 (*ortho-CH-OCH*₂Ph), 133.2 (q, $^3J_{\text{BC}} = 2.9\text{ Hz}$, *meta-C-B*(3,5-Me₂-C₆H₃)₄), 135.7 (*ortho-CH-B*(3,5-Me₂-C₆H₃)₄), 165.9 (q, $^1J_{\text{BC}} = 49.2\text{ Hz}$, *ipso-C-B*(3,5-Me₂-

C₆H₃)₄) ppm. ¹¹B{¹H} NMR (THF-*d*₈; 128.4 MHz): δ -7.02 ppm. Anal. calc. for C₅₁H₇₁N₄BOMg (791.27 g·mol⁻¹): C, 77.41; H, 9.04; N, 7.08; Mg, 3.07. Found: C, 76.73; H, 9.63; N, 7.25; Mg, 3.33%.

¹H, ¹³C{¹H}, and ¹¹B{¹H} NMR spectra of [(Me₄TACD)Mg(OCH₂Ph)][B(3,5-Me₂-C₆H₃)₄] (6)

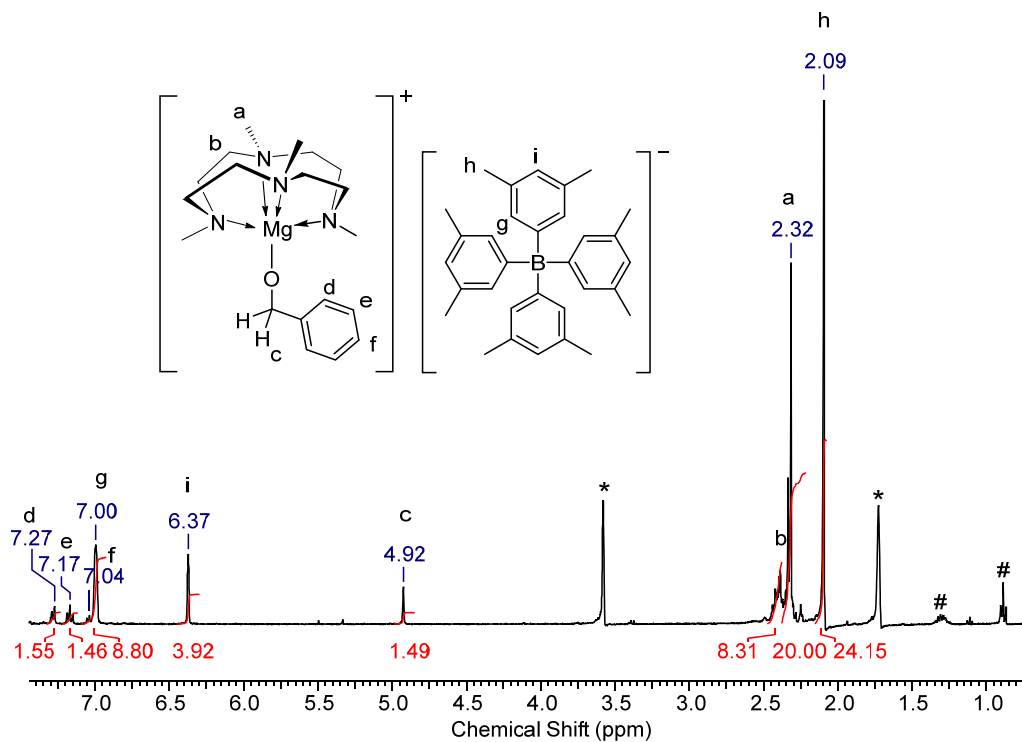


Figure S26. ¹H NMR spectrum of 6 in THF-*d*₈ (*) at 25 °C (*n*-pentane).

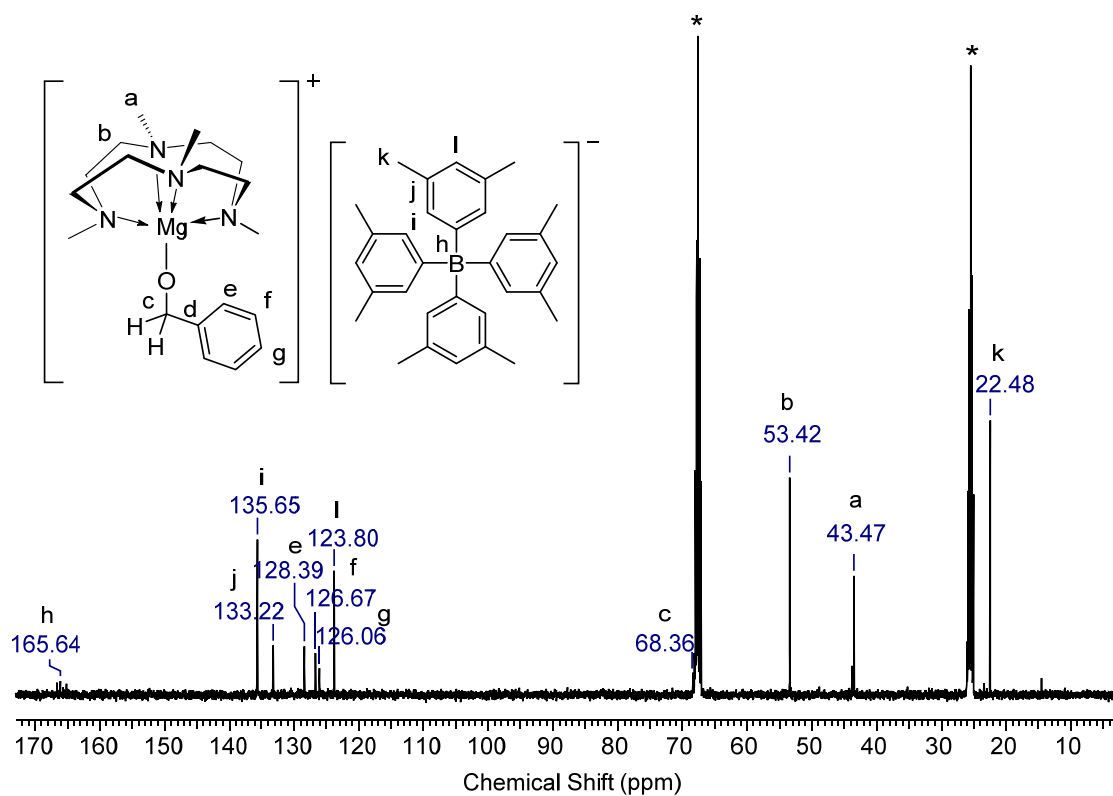


Figure S27. $^{13}\text{C}\{^1\text{H}\}$ NMR spectrum of **6** in THF- d_8 (*) at 25 °C.

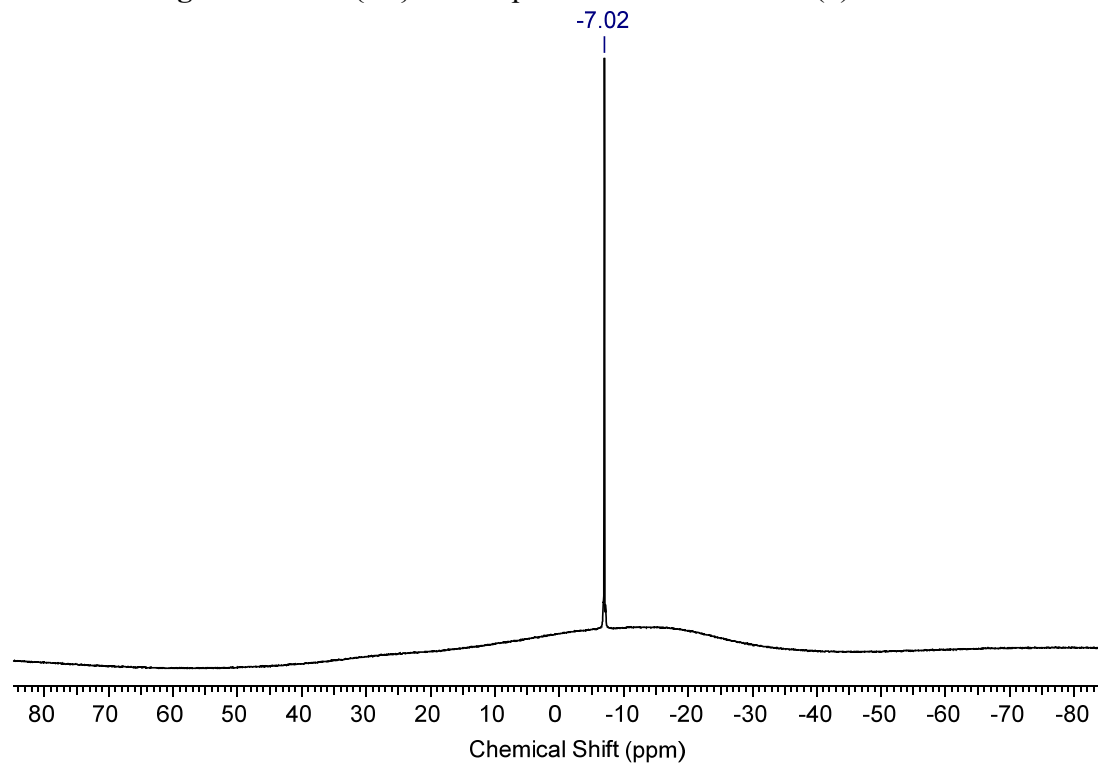


Figure S28. $^{11}\text{B}\{^1\text{H}\}$ NMR spectrum of **6** in THF- d_8 at 25 °C.

[(Me₄TACD)Mg(OCHPh₂)][B(3,5-Me₂-C₆H₃)₄] (7).** To a solution of [(Me₄TACD)₂Mg(μ-H)₂][B(3,5-Me₂-C₆H₃)₄]₂ (**2**) (68 mg, 0.05 mmol) in THF (4 mL) was added a solution of benzophenone (18 mg, 0.1 mmol) in THF (1 mL) at room temperature and the reaction mixture was stirred for 10 min. The solvent was removed under reduced pressure and the colorless solid residue was washed with diethyl ether (6 mL) and *n*-pentane (4.5 mL). The solid was dried under vacuum to give [(Me₄TACD)Mg(OCHPh₂)]**[B(3,5-Me₂-C₆H₃)₄] (7)** (74 mg, 0.08 mmol) in 85% yield. ¹H NMR (THF-*d*₈; 400.1 MHz): δ 2.09 (s, 24H, CH₃-B(3,5-Me₂-C₆H₃)₄), 2.21 (s, 12H, CH₃-Me₄TACD), 2.21 - 2.30 (m, 8H, CH₂-Me₄TACD), 2.33 - 2.40 (m, 8H, CH₂-Me₄TACD), 5.90 (OCHPh₂), 6.37 (m, 4H, *para*-CH-B(3,5-Me₂-C₆H₃)₄), 6.99 (m, 8H, *ortho*-CH-B(3,5-Me₂-C₆H₃)₄), 7.01 (m, 2H, *para*-CH-Ph), 7.13 (m, 4H, *meta*-CH-Ph), 7.35 (m, 4H, *ortho*-CH-Ph) ppm. ¹³C{¹H} NMR (THF-*d*₈; 100.6 MHz): δ 22.5 (CH₃-B(3,5-Me₂-C₆H₃)₄), 25.3 (s, 12H, CH₃-Bpin, identified by HSQC), 43.7 (CH₃-Me₄TACD), 53.4 (CH₂-Me₄TACD), 123.8 (*para*-CH-B(3,5-Me₂-C₆H₃)₄), 126.3 (*para*-CH-Ph), 127.3 (*ortho*-CH-Ph), 128.4 (*meta*-CH-Ph), 133.2 (q, ³J_{BC} = 2.9 Hz, *meta*-C-B(3,5-Me₂-C₆H₃)₄), 135.7 (*ortho*-CH-B(3,5-Me₂-C₆H₃)₄), 153.9 (*ipso*-C-Ph), 165.9 (q, ¹J_{BC} = 49.2 Hz, *ipso*-C-B(3,5-Me₂-C₆H₃)₄) ppm. ¹¹B{¹H} NMR (THF-*d*₈; 128.4 MHz): δ -7.00 ppm. Anal. calc. for C₅₇H₇₅N₄BOMg (867.37 g·mol⁻¹): C, 78.93; H, 8.72; N, 6.46; Mg, 2.80. Found: C, 76.68; H, 8.51; N, 6.17; Mg, 2.86 %.**

^1H , $^{13}\text{C}\{^1\text{H}\}$, and $^{11}\text{B}\{^1\text{H}\}$ NMR spectra of $[(\text{Me}_4\text{TACD})\text{Mg}(\text{OCHPh}_2)][\text{B}(3,5\text{-Me}_2\text{-C}_6\text{H}_3)_4]$ (**7**)

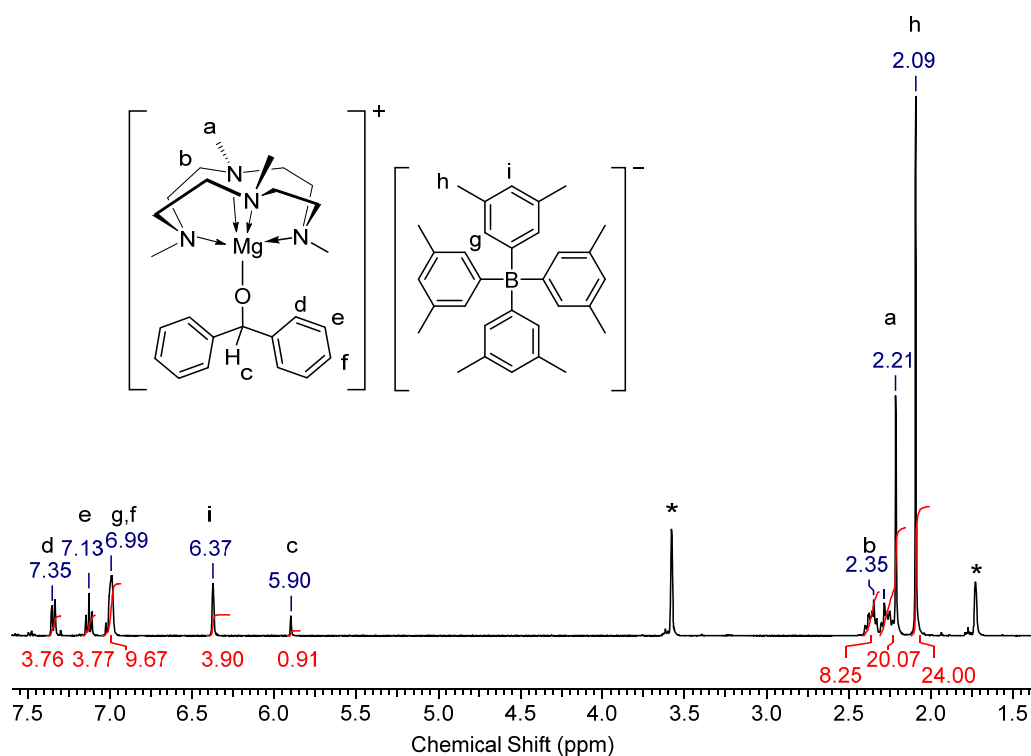


Figure S29. ^1H NMR spectrum of **7** in $\text{THF-}d_8$ (*) at 25°C .

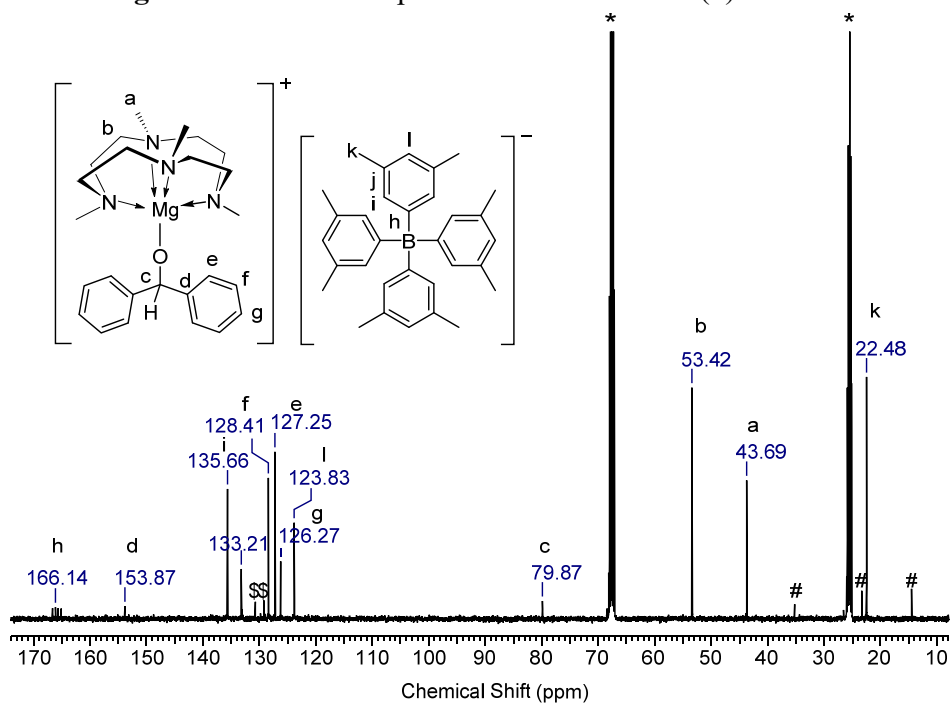


Figure S30. $^{13}\text{C}\{^1\text{H}\}$ NMR spectrum of **7** in $\text{THF-}d_8$ (*) at 25°C (# *n*-pentane, \$ unidentified species).

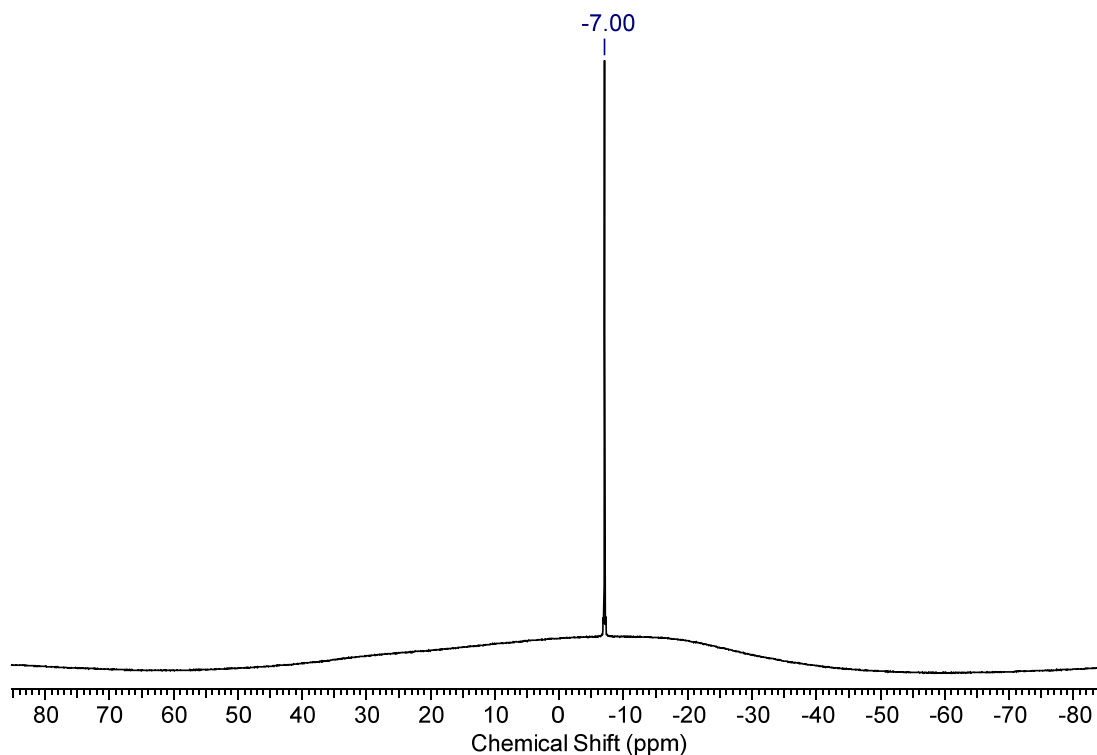


Figure S31. $^{11}\text{B}\{^1\text{H}\}$ NMR spectrum of **7** in THF- d_8 at 25 °C.

[(Me₄TACD)Mg(1,2-DHP)][B(3,5-Me₂-C₆H₃)₄] (8a**).** To a solution of [(Me₄TACD)₂Mg(μ-H)₂][B(3,5-Me₂-C₆H₃)₄]₂ (**2**) (103 mg, 0.05 mmol) in THF (4 mL) was added a solution of neat pyridine (12 μL, 12 mg, 0.1 mmol) and the reaction mixture was stirred for 2 h at 50 °C. The solvent was removed under reduced pressure and the colorless solid residue was washed with *n*-pentane (9 mL). The solid was dried under vacuum to give [(Me₄TACD)Mg(1,2-DHP)][B(3,5-Me₂-C₆H₃)₄] (**8a**) (100 mg, 0.13 mmol) as slightly yellow powder in 87% yield. Crystals suitable for X-ray analysis were obtained from layering a highly concentrated THF solution with benzene. ^1H NMR (THF- d_8 ; 400.1 MHz): δ 2.10 (s, 24H, CH₃-B(3,5-Me₂-C₆H₃)₄), 2.30-2.44 (m, 16H, CH₂-Me₄TACD), 2.35 (s, 12H, CH₃-Me₄TACD), 3.46 (d, 2H, $^3J_{\text{HH}} = 4.3$ Hz, 2H-NC₅H₆), 4.21 (dtdd, 1H, $^3J_{\text{HH}} = 8.3$ Hz, $^3J_{\text{HH}} = 4.3$ Hz, $^4J_{\text{HH}} = 1.5$ Hz, $^5J_{\text{HH}} = 0.8$ Hz, 3H-NC₅H₆), 4.72 (ddd, 1H, $^3J_{\text{HH}} = 5.5$ Hz, $^3J_{\text{HH}} = 6.0$ Hz, $^4J_{\text{HH}} = 1.5$ Hz, 5H-NC₅H₆), 5.76 (dd, 1H, $^3J_{\text{HH}} = 8.3$ Hz, $^3J_{\text{HH}} = 5.5$ Hz, 4H-NC₅H₆), 6.38 (m, 4H, *para*-CH-B(3,5-Me₂-C₆H₃)₄), 6.45 (dd, 1H, $^3J_{\text{HH}} = 6.0$ Hz, $^5J_{\text{HH}} = 0.8$ Hz, 6H-NC₅H₆), 7.00 (m, 8H, *ortho*-CH-B(3,5-Me₂-C₆H₃)₄) ppm. $^{13}\text{C}\{^1\text{H}\}$ NMR (THF- d_8 ; 100.6 MHz): δ 22.5 (CH₃-[B(3,5-Me₂-C₆H₃)₄]), 43.8 (CH₃-Me₄TACD), 48.9 (1C-NC₅H₆), 53.7 (CH₂-Me₄TACD), 69.1 (2C-NC₅H₆), 69.4 (4C-NC₅H₆), 123.9 (*para*-CH-B(3,5-Me₂-C₆H₃)₄), 128.1 (3C-

NC₅H₆), 133.3 (q, ³J_{BC} = 2.9 Hz, *meta*-C-B(3,5-Me₂-C₆H₃)₄), 135.7 (*ortho*-CH-B(3,5-Me₂-C₆H₃)₄), 148.7 (5C-NC₅H₆), 165.9 (q, ¹J_{BC} = 49.2 Hz, *ipso*-C-B(3,5-Me₂-C₆H₃)₄) ppm. ¹¹B{¹H}-NMR (THF-*d*₈; 128.4 MHz): δ -7.02 ppm. Anal. calc. for C₄₉H₇₀N₅BMg (764.25 g·mol⁻¹): C, 77.01; H, 9.23; N, 9.16; Mg, 3.18. Found: C, 74.77; H, 8.81; N, 8.92; Mg, 2.72 %.

¹H, ¹³C{¹H}, and ¹¹B{¹H} NMR spectra of [(Me₄TACD)Mg(1,2-DHP)][B(3,5-Me₂-C₆H₃)₄] (**8a**)

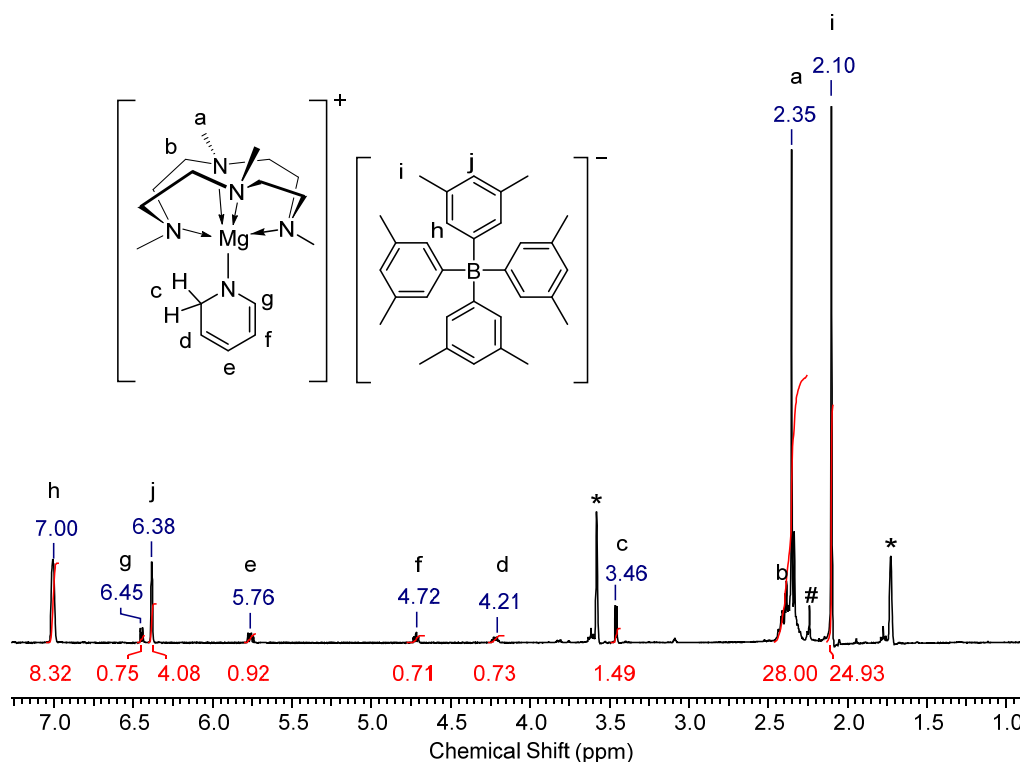


Figure S32. ¹H NMR spectrum of **8a** in THF-*d*₈ (*) at 25 °C.

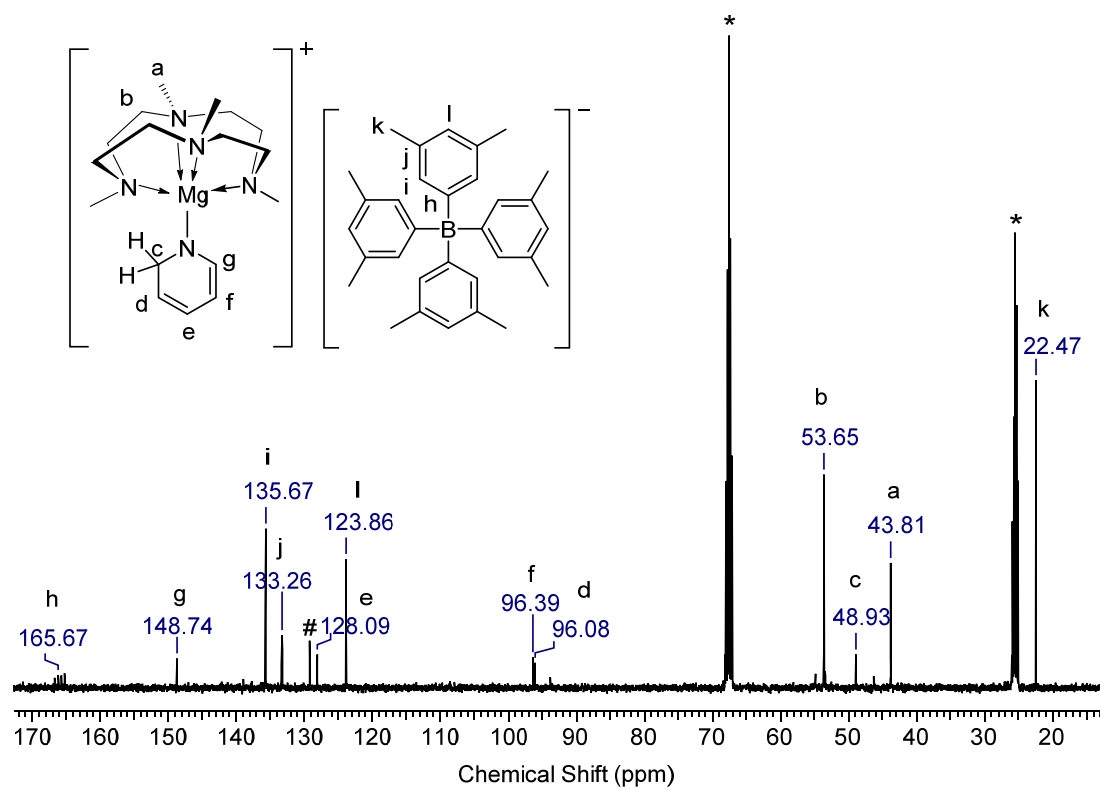


Figure S33. $^{13}\text{C}\{^1\text{H}\}$ NMR spectrum of **8a** in $\text{THF-}d_8$ (*) at 25 °C (# benzene).

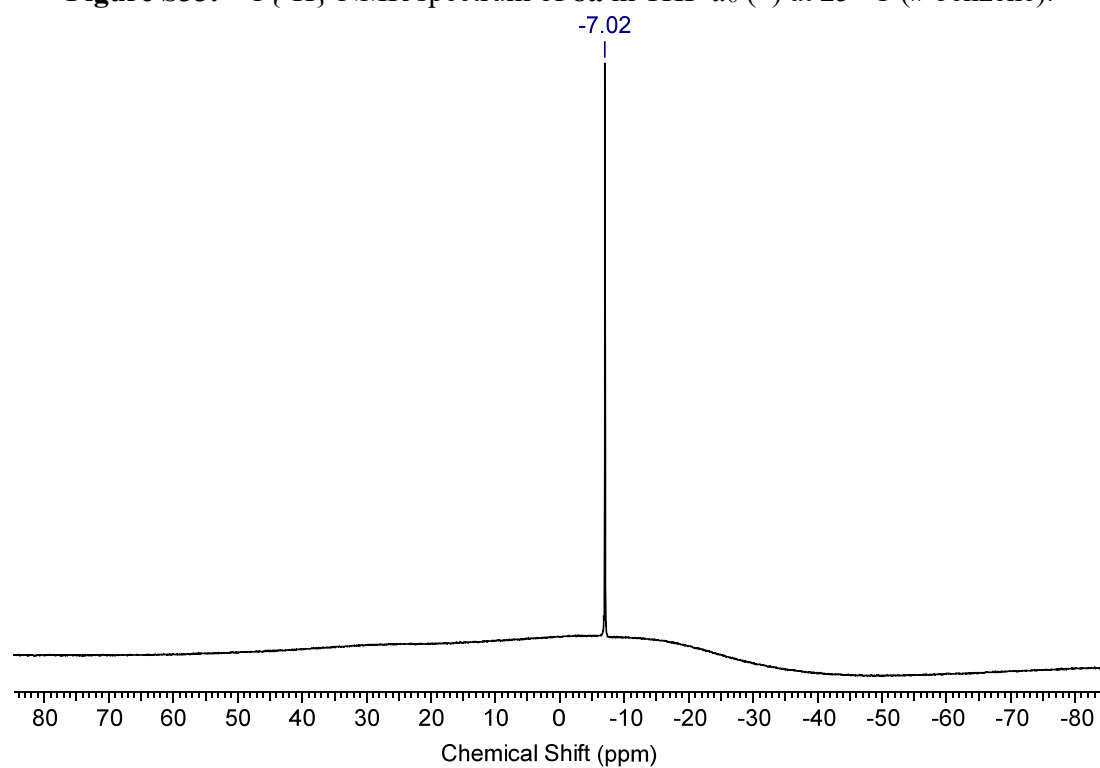


Figure S34. $^{11}\text{B}\{^1\text{H}\}$ NMR spectrum of **8a** in $\text{THF-}d_8$ at 25 °C.

[(Me₄TACD)Mg(1,4-DHP)][B(3,5-Me₂-C₆H₃)₄] (8b). To a solution of [(Me₄TACD)Mg(1,2-DHP)][B(3,5-Me₂-C₆H₃)₄] (**2**) (76 mg, 0.1 mmol) in THF (5 mL) a solution of [Mg(THF)₆][B(3,5-Me₂-C₆H₃)₄]₂ (**9**) (13 mg, 0.01 mmol; 10 mol%) was added and the reaction mixture was heated to 70 °C for 4 h. The solvent was removed under reduced pressure and the colorless solid residue was washed with *n*-pentane (3 x 3 mL). The solid was dried under vacuum and was crystallized from THF/cyclohexane at -30 °C over a period of 3 days to give [(Me₄TACD)Mg(1,4-DHP)][B(3,5-Me₂-C₆H₃)₄] (**8b**) (65 mg, 0.08 mmol) as colorless powder in 85% yield. ¹H NMR (THF-*d*₈; 400.1 MHz): δ 2.10 (s, 24H, CH₃-B(3,5-Me₂-C₆H₃)₄), 2.23 - 2.41 (m, 16H, CH₂-Me₄TACD), 2.33 (s, 12H, CH₃-Me₄TACD), 3.09 (m, 2H, 4*H*-NC₅H₆), 3.83 (m, 2H, 3*H*-NC₅H₆), 5.78 (m, 2H, 2*H*-NC₅H₆), 6.38 (m, 4H, *para*-CH-B(3,5-Me₂-C₆H₃)₄), 7.01 (m, 8H, *ortho*-CH-B(3,5-Me₂-C₆H₃)₄) ppm. ¹³C{¹H} NMR (THF-*d*₈; 100.6 MHz): δ 22.5 (CH₃-B(3,5-Me₂-C₆H₃)₄), 43.9 (CH₃-Me₄TACD), 25.5 (4*C*-NC₅H₆; overlapped by THF-*d*₈ signal but identified by HSQC), 53.6 (CH₂-Me₄TACD), 93.8 (3*C*-NC₅H₆), 123.9 (*para*-CH-B(3,5-Me₂-C₆H₃)₄), 133.3 (q, ³*J*_{BC} = 2.9 Hz, *meta*-C-B(3,5-Me₂-C₆H₃)₄), 135.7 (*ortho*-CH-B(3,5-Me₂-C₆H₃)₄), 138.9 (2*C*-NC₅H₆), 165.9 (q, ¹*J*_{BC} = 49.2 Hz, *ipso*-C-B(3,5-Me₂-C₆H₃)₄) ppm. ¹¹B{¹H} NMR (THF-*d*₈; 128.4 MHz): δ -7.00 ppm. Anal. calc. for C₄₉H₇₀N₅BMg (764.25 g·mol⁻¹): C, 77.01; H, 9.23; N, 9.16; Mg, 3.18. Found: C, 74.09; H, 9.10; N, 8.80.

¹H, ¹³C{¹H}, and ¹¹B{¹H} NMR spectra of [(Me₄TACD)Mg(1,4-DHP)][B(3,5-Me₂-C₆H₃)₄] (8b)

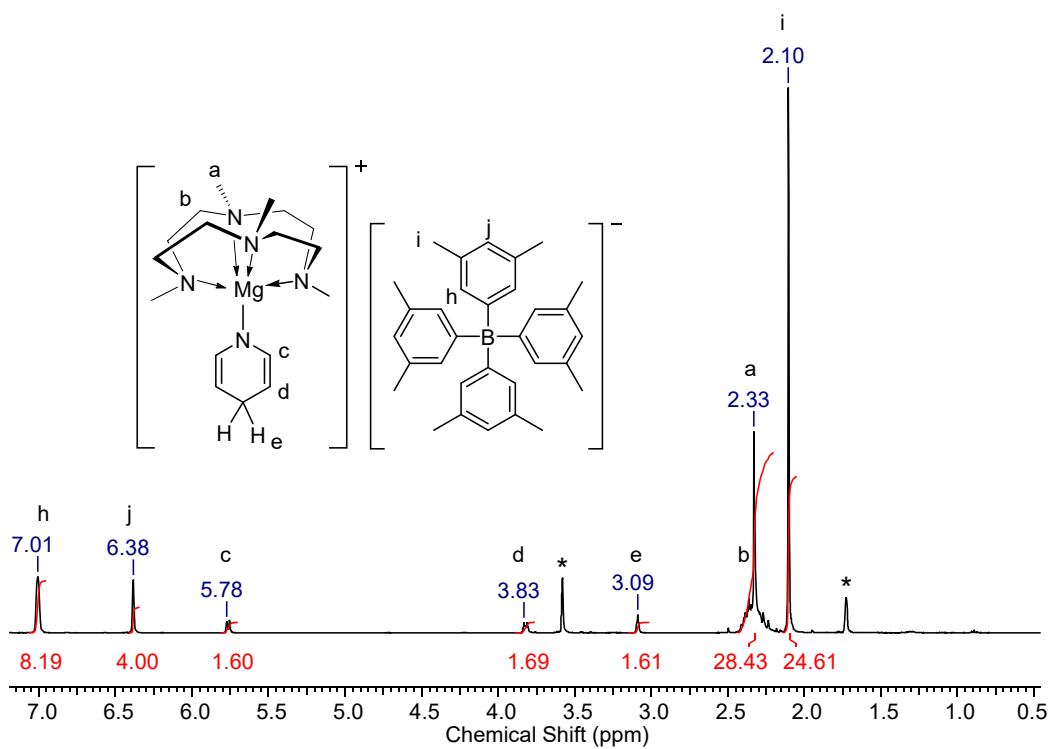


Figure S35. ^1H NMR spectrum of **8b** in THF-d_8 (*) at 25°C .

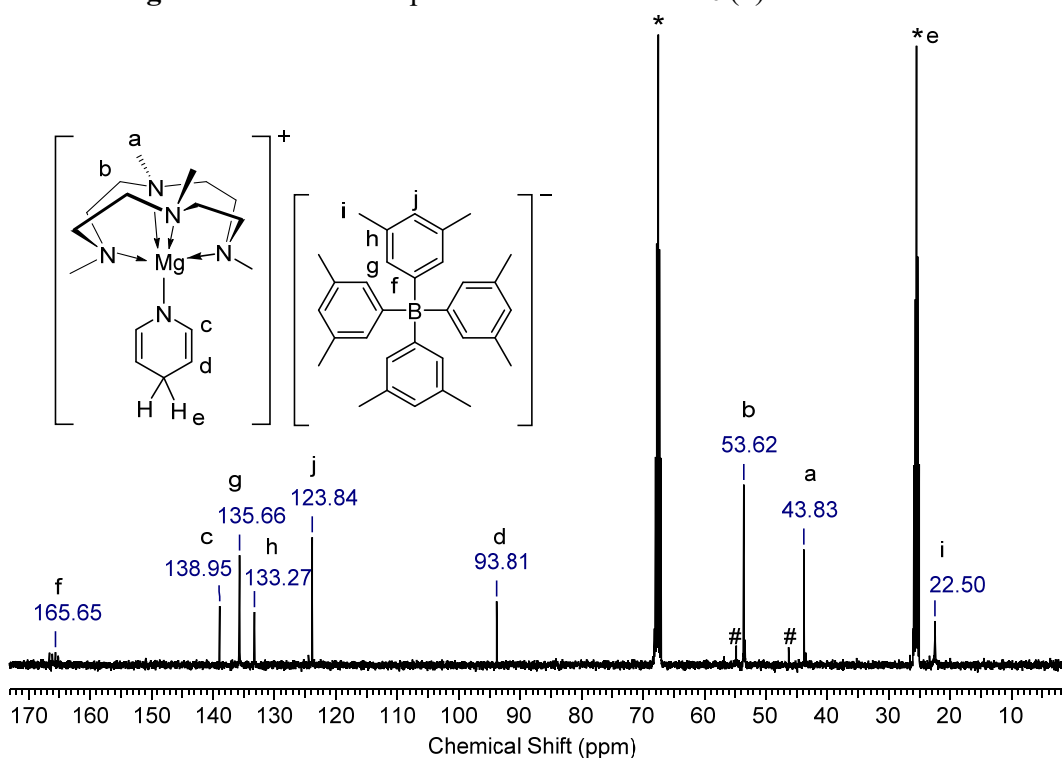


Figure S36. $^{13}\text{C}\{^1\text{H}\}$ NMR spectrum of **8b** in THF-d_8 (*) at 25°C (# unidentified species).

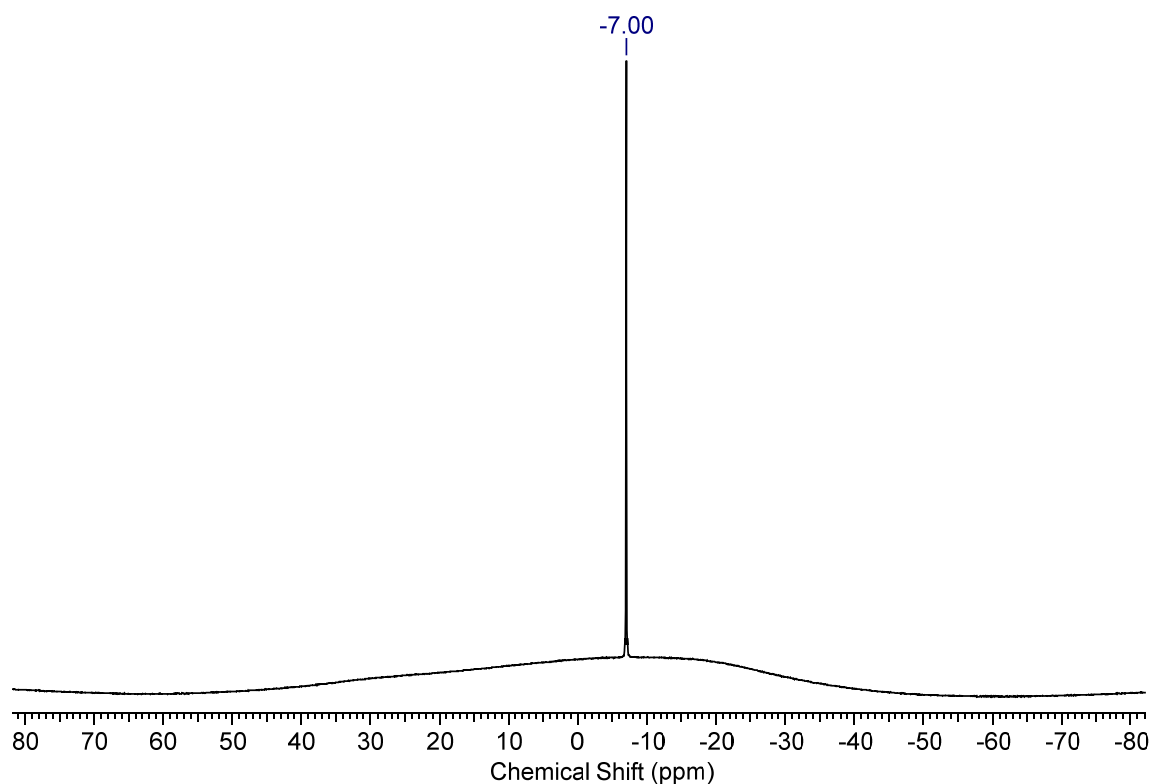


Figure S37. $^{11}\text{B}\{^1\text{H}\}$ NMR spectrum of **8b** in THF- d_8 at 25 °C.

[Mg(THF)₆][B(3,5-Me₂-C₆H₃)₄]₂ (9). To a solution of [Mg^tBu₂]^[7] (14 mg; 0.1 mmol) in THF (2 mL) a suspension of [NEt₃H][B(3,5-Me₂-C₆H₃)₄] (107 mg, 0.2 mmol) was added and the reaction mixture was stirred for 16 h at room temperature. The solvent was removed under vacuum and the colorless residue was washed with *n*-pentane (3 mL). The solvent was dried under vacuum and [Mg(THF)₆][B(3,5-Me₂-C₆H₃)₄]₂ (**9**) (98 mg, 0.07 mmol) was obtained in 74% yield. ¹H NMR (THF- d_8 ; 400.1 MHz): δ = 2.08 (s, 48H, CH₃-B(3,5-Me₂-C₆H₃)₄), 6.35 (m, 8H, *para*-CH-B(3,5-Me₂-C₆H₃)₄), 6.96 (m, 16H, *ortho*-CH-B(3,5-Me₂-C₆H₃)₄) ppm. ¹³C{¹H} NMR (THF- d_8 ; 100.6 MHz): δ = 22.5 (CH₃-[B(3,5-Me₂-C₆H₃)₄]), 123.6 (*para*-CH-B(3,5-Me₂-C₆H₃)₄), 133.0 (q, ³J_{BC} = 2.9 Hz, *meta*-C-B(3,5-Me₂-C₆H₃)₄), 135.6 (*ortho*-CH-B(3,5-Me₂-C₆H₃)₄), 165.8 (q, ¹J_{BC} = 49.2 Hz, *ipso*-C-B(3,5-Me₂-C₆H₃)₄) ppm. ¹¹B{¹H} NMR (THF- d_8 ; 128.4 MHz): δ = -6.93 ppm. Anal. calcd. for C₈₈H₁₂₀B₂O₆Mg (1319.85 g·mol⁻¹): C, 80.08; H, 9.16; Mg, 1.84. Found: C, 78.76; H, 9.24.

^1H , $^{13}\text{C}\{^1\text{H}\}$, and $^{11}\text{B}\{^1\text{H}\}$ NMR spectra of $[\text{Mg}(\text{THF})_6][\text{B}(\text{3,5-Me}_2\text{-C}_6\text{H}_3)_4]_2$ (**9**)

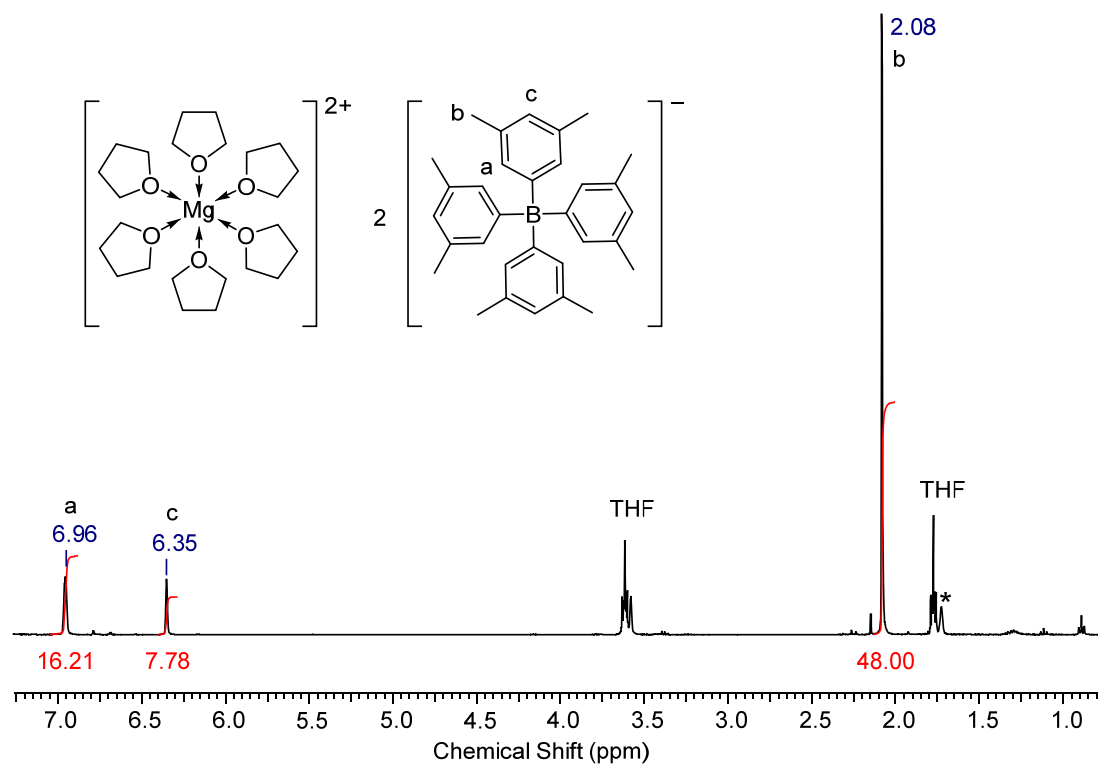


Figure S38. ^1H NMR spectrum of **9** in $\text{THF-}d_8$ (*) at 25 °C.

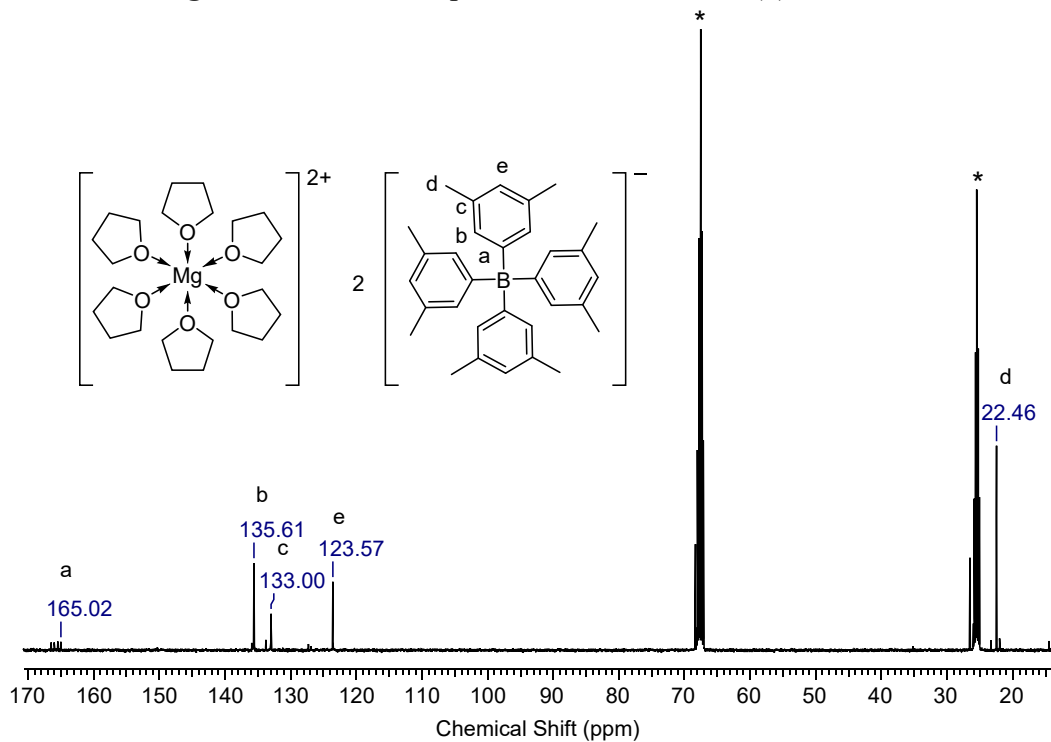


Figure S39. $^{13}\text{C}\{^1\text{H}\}$ NMR spectrum of **9** in $\text{THF-}d_8$ (*) at 25 °C.

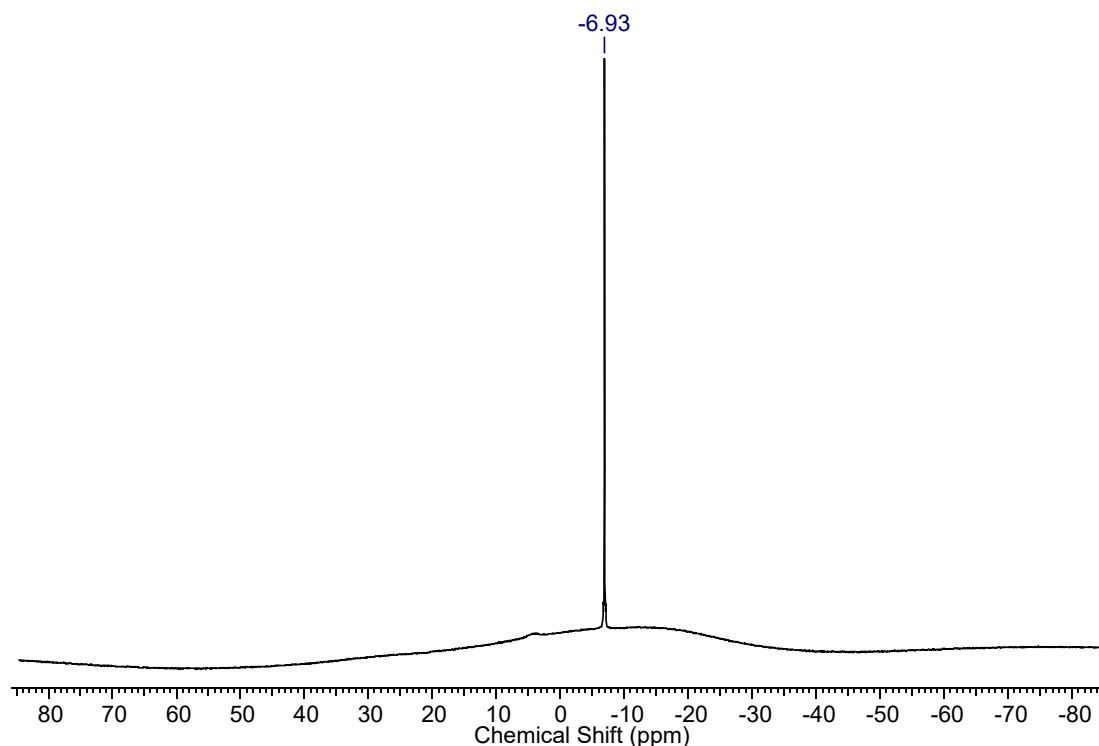


Figure S40. $^{11}\text{B}\{^1\text{H}\}$ NMR spectrum of **9** in $\text{THF-}d_8$ at $25\text{ }^\circ\text{C}$.

Solid state structure of $[\text{Mg}(\text{THF})_6][\text{B}(3,5\text{-Me}_2\text{-C}_6\text{H}_3)_4]_2$ (9**).**

Single crystals of $[\text{Mg}(\text{THF})_6][\text{B}(3,5\text{-Me}_2\text{-C}_6\text{H}_3)_4]_2$ (**9**) were obtained from a THF/*n*-hexane mixture at $-30\text{ }^\circ\text{C}$ over a period of 16 h. **9** displays a solvent separated ion pair containing a cationic magnesium centre coordinated by six oxygen atoms and two $[\text{B}(3,5\text{-Me}_2\text{-C}_6\text{H}_3)_4]$ anions. The structure of $[\text{Mg}(\text{THF})_6][\text{B}(3,5\text{-Me}_2\text{-C}_6\text{H}_3)_4]_2$ (**9**) is similar to that of $[\text{Mg}(\text{THF})_6][\text{BPh}_4]_2$.^[8] The only difference is that herein each solvated cation is surrounded by a framework of four instead of eight borate anions due to the higher steric demand of the $[\text{B}(3,5\text{-Me}_2\text{-C}_6\text{H}_3)_4]$ anion compared to the $[\text{BPh}_4]$ anion (Figure S41).

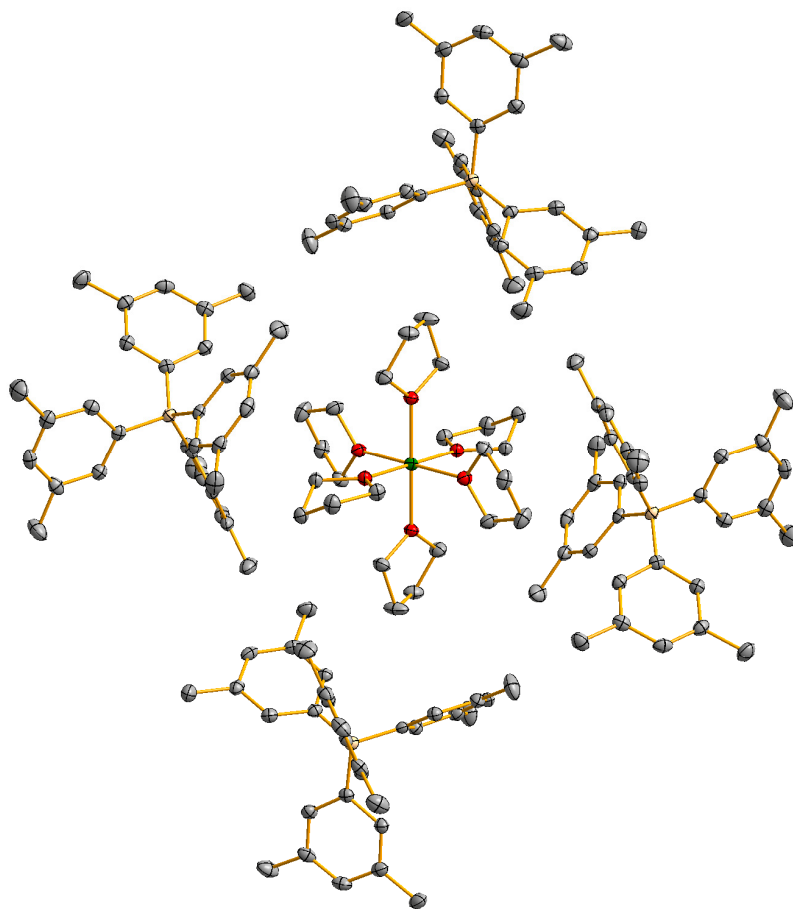


Figure S41. Packing of anions and cations in the crystal structure of $[\text{Mg}(\text{THF})_6][\text{B}(3,5\text{-Me}_2\text{-C}_6\text{H}_3)_4]_2$ (**9**). Displacement parameters are shown at the 50% probability level. Hydrogen atoms are omitted for clarity.

Isomerization of $[(\text{Me}_4\text{TACD})\text{Mg}(1,2\text{-DHP})][\text{B}(3,5\text{-Me}_2\text{-C}_6\text{H}_3)_4]$ (8a**) into $[(\text{Me}_4\text{TACD})\text{Mg}(1,4\text{-DHP})][\text{B}(3,5\text{-Me}_2\text{-C}_6\text{H}_3)_4]$ (**8b**) in the presents of $[\text{Mg}(\text{THF})_6][\text{B}(3,5\text{-Me}_2\text{-C}_6\text{H}_3)_4]_2$ (**9**) in THF-*d*₈ at 70 °C.**

To investigate the reaction of **8a** into **8b** in the presents of $[\text{Mg}(\text{THF})_6][\text{B}(3,5\text{-Me}_2\text{-C}_6\text{H}_3)_4]_2$ (**9**) in THF-*d*₈ samples with $[(\text{Me}_4\text{TACD})\text{Mg}(1,2\text{-DHP})][\text{B}(3,5\text{-Me}_2\text{-C}_6\text{H}_3)_4]$ (**8a**) (7.6 mg; 0.01 mmol), $[\text{Mg}(\text{THF})_6][\text{B}(3,5\text{-Me}_2\text{-C}_6\text{H}_3)_4]_2$ (**9**) (1.3 mg; 0.001 mmol; 10 mol%) and hexamethylbenzene (internal standard: 1.6 mg; 0.01 mmol) in THF-*d*₈ (0.5 mL) were prepared. The samples were heated up to 70 °C and the conversion of **8a** into **8b** was monitored by ¹H NMR spectroscopy. The plot of the concentration of **8a** versus time is shown in Figure S42. The reaction follows a zero order kinetics and a reaction rate of $k = (1.64 \pm 0.06) \cdot 10^{-6} \text{ mol} \cdot \text{L}^{-1} \cdot \text{s}^{-1}$ is determined.

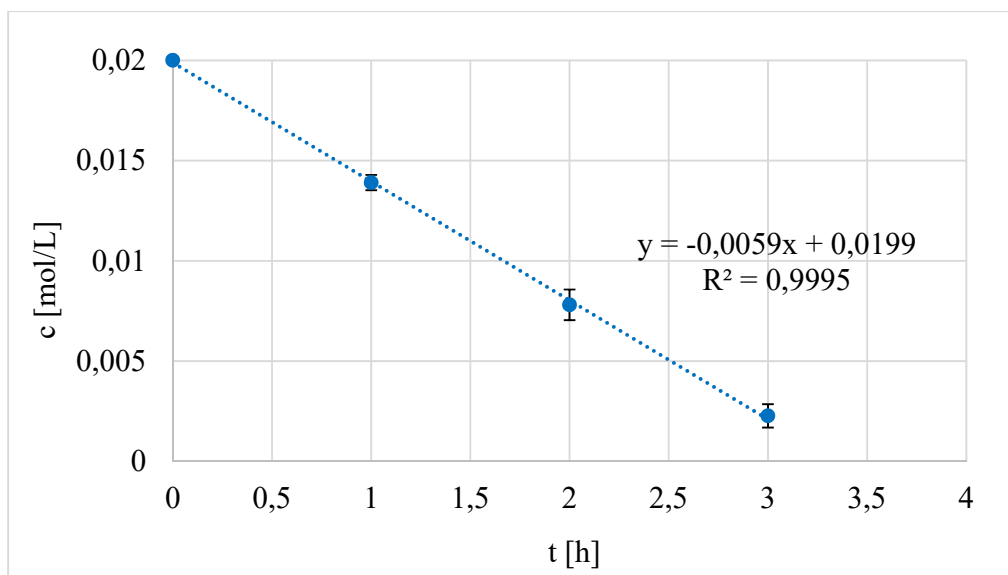


Figure S42. Plot of the concentration of **8a** versus time in THF-*d*₈ at 343 K.

Exchange reactions of [(Me₄TACD)Mg(1,2-DHP)][B(3,5-Me₂-C₆H₃)₄] (8a**) and [(Me₄TACD)Mg(1,4-DHP)][B(3,5-Me₂-C₆H₃)₄] (**8b**) in pyridine-*d*₅.**

To investigate the reactions of **8a** and **8b** with pyridine-*d*₅ samples with [(Me₄TACD)Mg(1,2-DHP)][B(3,5-Me₂-C₆H₃)₄] (**8a**) or [(Me₄TACD)Mg(1,4-DHP)][B(3,5-Me₂-C₆H₃)₄] (**8b**) (7.6 mg; 0.01 mmol) and hexamethylbenzene (internal standard: 1.6 mg; 0.01 mmol) in pyridine-*d*₅ (0.5 mL) were prepared. **8a** and **8b** show slow exchange in pyridine-*d*₅ at 70 °C under the formation of a mixed deuterohydropyridyl species (**8a-4H-*d*₅** and **8b-4H-*d*₅**). Further reaction to the completely deuterated species (**8a-*d*₆** and **8b-*d*₆**) proceeded over time. The products **8b-4H-*d*₅** and **8b-*d*₆** are identified by ¹H and ²D NMR spectroscopy (Figure S43).

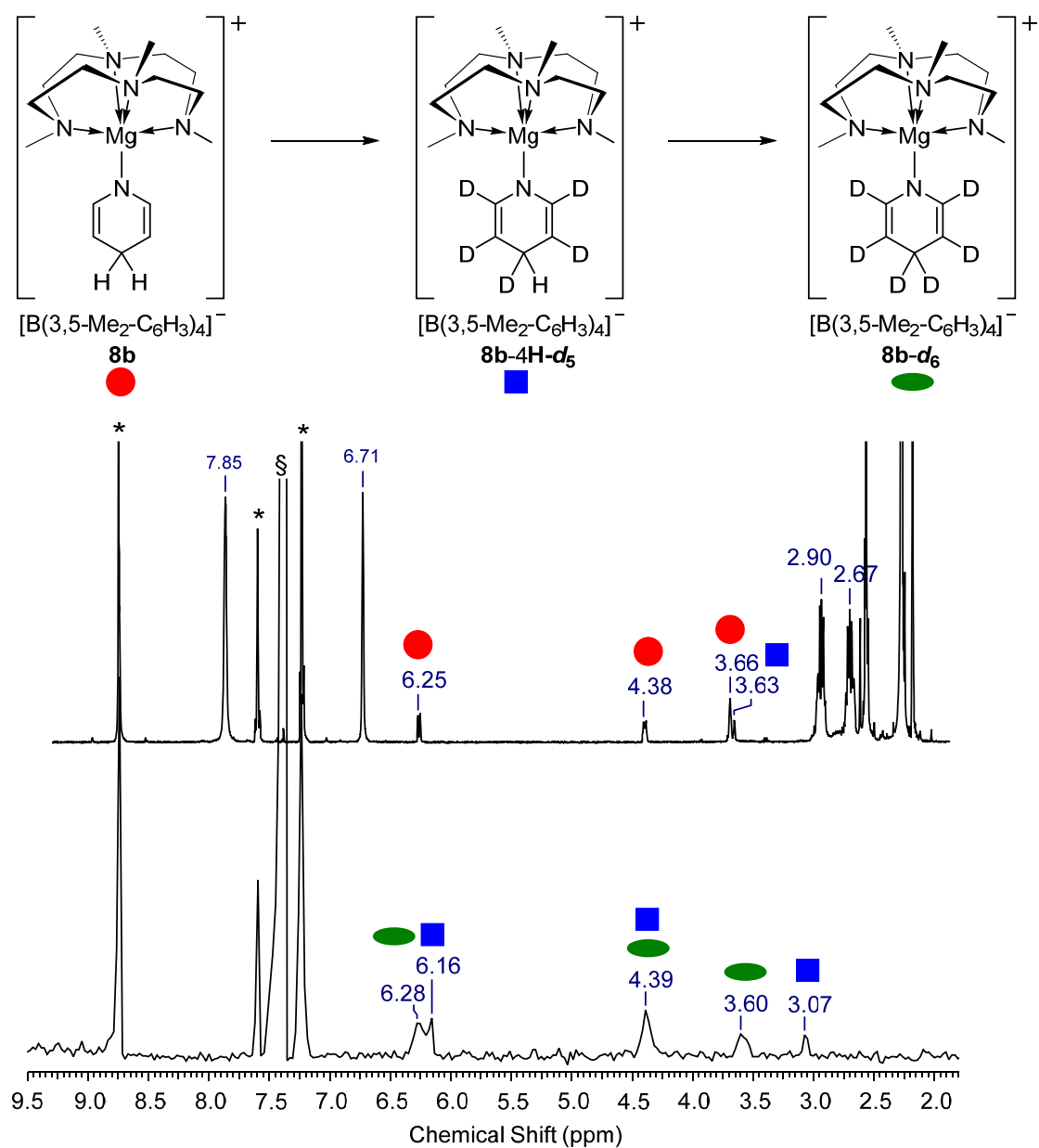


Figure S43. ^1H NMR spectrum of $[(\text{Me}_4\text{TACD})\text{Mg}(1,4\text{-DHP})][\text{B}(3,5\text{-Me}_2\text{-C}_6\text{H}_3)_4]$ (**8b**) in pyridine- d_5 (*) after 17 h at 70 °C (top) and ^2D NMR spectrum of the reaction of $[(\text{Me}_4\text{TACD})\text{Mg}(1,4\text{-DHP})][\text{B}(3,5\text{-Me}_2\text{-C}_6\text{H}_3)_4]$ (**8b**) in pyridine- d_5 after 5 days at 70 °C, dried and diluted in pyridine with benzene- d_6 (\$) as internal standard (bottom).

The amount of **8a** and **8b** in the reaction mixture was determined by ^1H NMR spectroscopy. The plot of $\ln(c/c_0)$ versus time is shown in Figure S44.

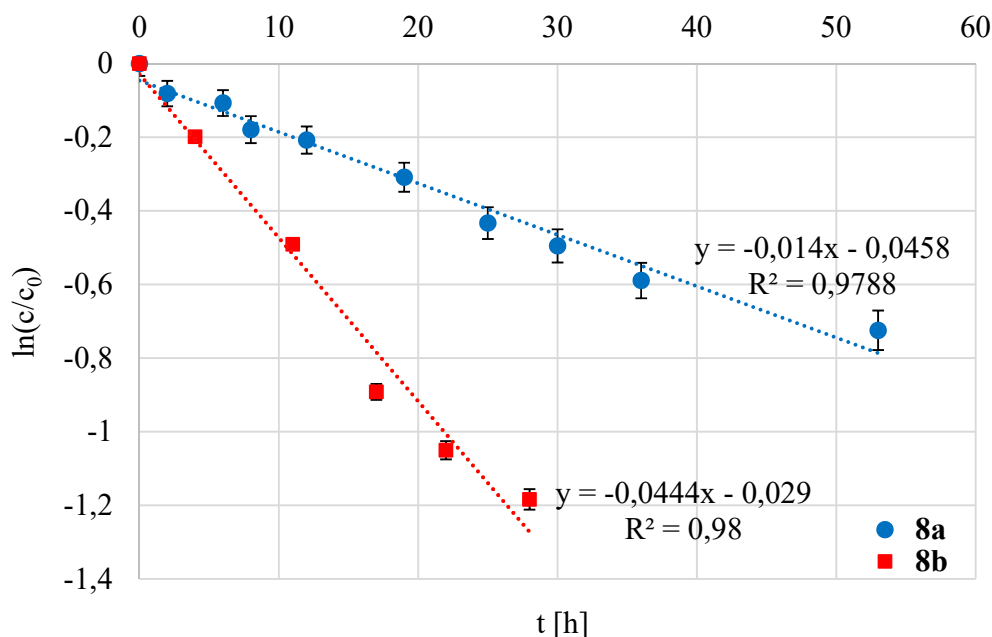


Figure S44. Plot of $\ln(c/c_0)$ versus time for the exchange of **8a** and **8b** in pyridine-*d*₅ at 343 K.

Crystal Structure Determinations

X-ray diffraction data were collected at -173 °C on a Bruker D8 goniometer with APEX CCD area-detector (**1**, **6**, **8a**) or on an Eulerian 4-circle diffractometer STOE STADIVARI (**2**, **3**, **4**, **9**) in ω -scan mode. All structures were solved by direct methods using SIR-97.^[9] The crystal lattice of **2** contains co-crystallized THF, the crystal of **4** contains THF as well as cyclohexane, the crystal of **8a** contains co-crystallized benzene. The structure of **9** reveals crystallographically imposed inversion symmetry for the cationic fragment $[\text{Mg}(\text{C}_4\text{H}_8\text{O})_6]^{2+}$ fragment with the atom Mg1 located on Wyckoff position $2a$.

All refinements were carried out against F^2 with SHELXL^[10] with anisotropic displacement parameters for the non-hydrogen atoms, as implemented in the program system WinGX.^[11] Hydrogen atoms were included in calculated positions and were treated as riding during the refinement. The hydride atoms of the central Mg_2H_2 fragment in **1** were located in a Fourier difference map and refined in their position. In **2**, related positions for the Mg_2H_2 hydrides were located in a single Fourier difference map with 0.64 and 0.71 $e\text{\AA}^3$, but their position could not be reliably refined due to the disorder in this data set. Using these positions for hydrogen atoms H1 and H2, refinement of their isotropic displacement parameters gave values that agree well with the other atoms of this structure. The hydrogen atoms of the BH_4 fragment in **3** (H1, H2, H3 and H4),

of the BH₂ unit in **4** (H1A and H1B), as well as of the C₅H₆B ring in **8a** (H13, H14, H15, H16, H17A, H17B) were refined in their position.

Disorder was revealed in the structure of **2**, where it was taken into account by split positions for the atoms C13 – C20 (methylene units) and C23, C24 (methyl units) of a Me₄TACD ligand, as well as for both co-crystallized THF ligands (C90, as well as O2, C93 – C96). The split positions within the THF molecules were refined with isotropic displacement parameters. Attempted refinement with anisotropic parameters did not lead to physically meaningful values. Due to the pronounced disorder within one of these THF molecules, same distance restraints (SAME instruction within the program SHELXL) were used in the refinement. The crystal structure of **9** shows a small disorder within a THF ligand coordinated to the metal centre that could be resolved by split positions for the positions of C10 and C11.

In the refinement of the crystal structure of **2**, twinning was taken into account by a twin rotation matrix (-1 0 0, 0 1 0, 0 0 -1) relating two components with a batch scale factor (BASF) of 0.48766. Figure S45 shows the staggered conformation of the magnesium compound **2** in comparison to the previously described calcium complex [(Me₄TACD)₂Ca₂(μ-H)₂]²⁺ and the lutetium complex [(Me₄TACD)₂Lu₂(μ-H)₄]²⁺.^[12, 13]

Graphical representations were obtained with the program DIAMOND.^[14] CCDC-1891829 (**1**), CCDC-1891830 (**2**), CCDC-1891831 (**3**), CCDC-1891832 (**4**) and CCDC-1891833 (**6**), CCDC-1891834 (**8a**) and CCDC-189182935 (**9**) contain the supplementary crystallographic data for this paper. These data can be obtained free of charge from the Crystallographic Data Centre via www.ccdc.cam.ac.uk/data_request/cif.

Table S1. Crystallographic data of **1**, **2**, **3** and **4**.

	1	2	3	4
formula	C ₂₄ H ₆₆ Mg ₂ N ₆ Si ₄	C ₂₄ H ₅₈ Mg ₂ N ₈ , 2(C ₃₂ H ₃₆ B), 2(C ₄ H ₈ O)	C ₁₂ H ₃₂ BMgN ₄ , C ₃₂ H ₃₆ B	C ₃₂ H ₃₆ B, C ₁₈ H ₄₂ BMgN ₄ O ₂ , C ₆ H ₁₂ , 3(C ₄ H ₈ O)
<i>F</i> _w /g·mol ⁻¹	599.80	1514.44	698.95	1113.56
cryst. color, habit	colourless block	colourless plate	colourless rod	colourless plate
crystal size / mm	0.22 × 0.22 × 0.23	0.09 × 0.29 × 0.50	0.12 × 0.22 × 0.41	0.10 × 0.21 × 0.32
crystal system	monoclinic	orthorhombic	monoclinic	triclinic
space group	<i>P</i> 2 ₁ / <i>n</i> (no. 14)	<i>Pna</i> 2 ₁ (no. 33)	<i>P</i> 2 ₁ (no. 4)	<i>P</i> $\bar{1}$ (no. 2)
<i>a</i> / Å	12.029(3)	36.3501(5)	11.870(2)	12.0615(4)
<i>b</i> / Å	18.831(5)	12.34279(12)	15.682(3)	13.3505(5)
<i>c</i> / Å	17.330(5)	20.1258(2)	11.922(2)	21.4909(9)
α / °				83.123(3)
β / °	105.496(4)		90.00(3)	77.706(3)
γ / °				85.097(3)
<i>V</i> / Å ³	3782.9(18)	9029.67(18)	2219.2(7)	3350.5(2)
<i>Z</i>	4	4	2	2
<i>d</i> _{calc} /Mg·m ⁻³	1.053	1.114	1.046	1.104
μ /mm ⁻¹	0.212 (MoK α)	0.621 (CuK α)	0.575 (CuK α)	0.602 (CuK α)
<i>F</i> (000)	1328	3312	764	1224
ϑ range / °	1.63 – 30.60	4.33 – 71.89	4.67 – 68.24	4.68 – 71.47
index ranges	-17 ≤ <i>h</i> ≤ 17, -26 ≤ <i>k</i> ≤ 26, -24 ≤ <i>l</i> ≤ 24	-44 ≤ <i>h</i> ≤ 42, -14 ≤ <i>k</i> ≤ 4, -24 ≤ <i>l</i> ≤ 23	-14 ≤ <i>h</i> ≤ 7, -18 ≤ <i>k</i> ≤ 18, -14 ≤ <i>l</i> ≤ 13	-14 ≤ <i>h</i> ≤ 14, -16 ≤ <i>k</i> ≤ 15, -17 ≤ <i>l</i> ≤ 25
refln.	57115	63436	12825	21480
independ. reflns (<i>R</i> _{int})	11236 (0.0805)	16234 (0.0411)	6907 (0.0246)	11298 (0.0301)
observed reflns	8332	13365	6357	7647
data/ restr./ param.	11236 / 0 / 349	16234 / 28 / 1042	6907 / 1 / 488	11298 / 0 / 745
<i>R</i> ₁ , <i>wR</i> ₂ [<i>I</i> > 2 σ (<i>I</i>)]	0.0474, 0.1142	0.0597, 0.1572	0.0637, 0.1654	0.0891, 0.2600
<i>R</i> ₁ , <i>wR</i> ₂ (all data)	0.0717, 0.1248	0.0701, 0.1621	0.0698, 0.1732	0.1195, 0.2843
GooF on <i>F</i> ²	1.032	1.025	1.031	1.105
largest diff. peak, hole/ e·Å ³	0.722, -0.395	1.579, -0.286	0.440, -0.406	0.986, -0.588
CCDC number	1891829	1891830	1891831	1891832

Table S2. Crystallographic data of **6**, **8a** and **9**.

	6	8a	9
formula	C ₁₉ H ₃₅ MgN ₄ O, C ₃₂ H ₃₆ B	C ₁₇ H ₃₄ MgN ₅ , C ₃₂ H ₃₆ B, C ₆ H ₆	C ₁₁₂ H ₁₆₈ B ₂ MgO ₁₂
<i>F</i> w /g mol ⁻¹	791.23	842.32	1752.38
cryst. color, habit	colourless block	colourless block	colourless block
crystal size / mm	0.20 × 0.27 × 0.45	0.13 × 0.17 × 0.38	0.20 × 0.27 × 0.31
crystal system	orthorhombic	orthorhombic	monoclinic
space group	<i>P</i> 2 ₁ 2 ₁ 2 ₁ (no. 19)	<i>P</i> na2 ₁ (no. 33)	<i>P</i> 2 ₁ / <i>n</i> (no. 14)
<i>a</i> / Å	13.4152(10)	19.1374(13)	16.1902(3)
<i>b</i> / Å	16.7170(12)	11.8659(8)	17.9242(3)
<i>c</i> / Å	20.2430(16)	21.6820(15)	18.0628(4)
β / °			97.5641(16)
<i>V</i> / Å ³	4539.7(6)	4923.6(6)	5196.15(17)
<i>Z</i>	4	4	2
<i>d</i> _{calc} /Mg·m ⁻³	1.158	1.136	1.120
μ/mm ⁻¹	0.080 (MoKα)	0.077 (MoKα)	0.597 (CuKα)
<i>F</i> (000)	1720	1832	1916
ϑ range / °	1.58 – 23.29	1.88 - 25.42	4.64 – 70.96
index ranges	-14 ≤ <i>h</i> ≤ 14, -18 ≤ <i>k</i> ≤ 18, -22 ≤ <i>l</i> ≤ 22	-23 ≤ <i>h</i> ≤ 23, -14 ≤ <i>k</i> ≤ 14, -26 ≤ <i>l</i> ≤ 26	-19 ≤ <i>h</i> ≤ 15, -21 ≤ <i>k</i> ≤ 19, -20 ≤ <i>l</i> ≤ 17
refln.	42977	53696	24012
independ. reflns (<i>R</i> _{int})	6526 (0.0754)	9052 (0.0810)	9001 (0.0139)
observed reflns	5889	7332	7587
data/ restr./ param.	6526 / 0 / 535	9052 / 1 / 595	9001 / 0 / 601
<i>R</i> ₁ , <i>wR</i> ₂ [<i>I</i> > 2σ(<i>I</i>)]	0.0521, 0.1285	0.0488, 0.1086	0.0530, 0.1458
<i>R</i> ₁ , <i>wR</i> ₂ (all data)	0.0597, 0.1341	0.0674, 0.1184	0.0615, 0.1508
Goof on <i>F</i> ²	1.063	1.032	1.067
largest diff. peak, hole/ e ⁻ Å ³	0.763, -0.504	0.205, -0.164	0.972, -0.544
CCDC number	1891833	1891834	1891835

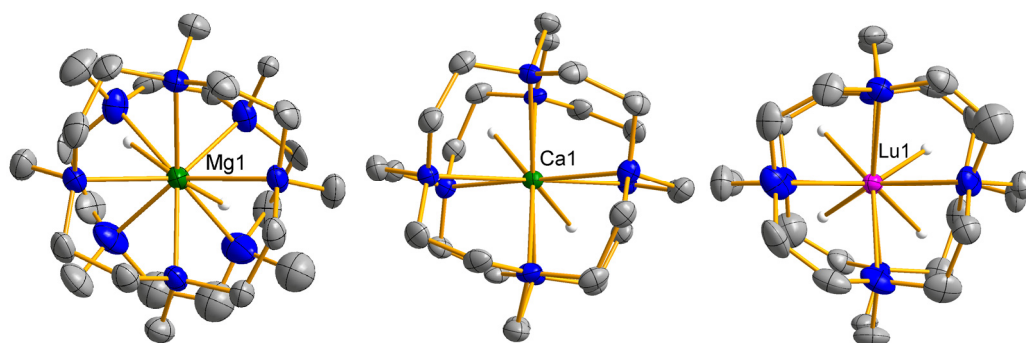


Figure S45. $[(\text{Me}_4\text{TACD})_2\text{Mg}_2(\mu\text{-H})_2]^{2+}$ (left), $[(\text{Me}_4\text{TACD})_2\text{Ca}_2(\mu\text{-H})_2]^{2+}$ (center) and $[(\text{Me}_4\text{TACD})_2\text{Lu}_2(\mu\text{-H})_4]^{2+}$ (right).^[12, 13]

DFT Calculations

Computational details

Quantum-chemical calculations: Geometry optimizations were performed with the Gaussian09 suite of programs (revision D.02)^[14] using the Becke's 3-parameter hybrid functional,^[15] combined with the non-local correlation functional provided by Perdew/Wang.^[16] The 6-311+G(d) all-electron basis set was used for the magnesium atom, and the 6-31G(d) for the remaining atoms.^[17] We have also considered in the present study the dispersion effects. In particular the third generation of Grimme's dispersion corrections with Becke-Johnson damping^[18] model on the B3PW91 geometries (single point calculations). All stationary points have been identified for minimum (Nimag = 0) Natural population analysis (NPA) was performed using Weinhold's methodology.^[19]

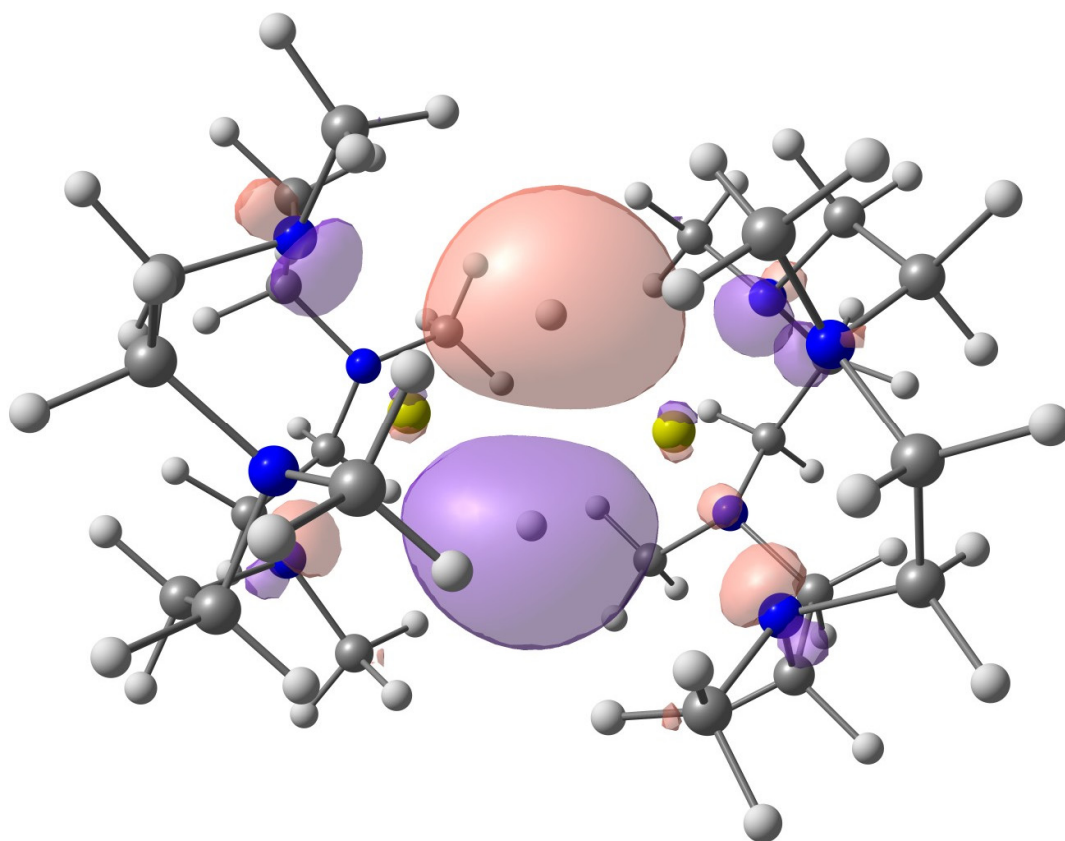


Figure S46. HOMO of the molecular dication $[(\text{Me}_4\text{TACD})_2\text{Mg}_2(\mu\text{-H})_2]^{2+}$ (**2**).

The HOMO of the molecular dication in the complex $[(\text{Me}_4\text{TACD})_2\text{Mg}_2(\mu\text{-H})_2][\text{B}(3,5\text{-Me}_2\text{-C}_6\text{H}_3)_4]_2$ clearly shows the bonding of the hydrides within the central Mg_2H_2 fragment. The disruption of the dimer by THF to give the associated monomers was computed to be favorable by 35.9 kcal/mol. In the absence of THF, the corresponding disruption is favored by 34.0 kcal/mol what indicates that the THF only has a minor stabilizing effect on the monomer.

Table S3. Cartesian coordinates of optimized structures

Dimer complex

Mg	13.629077000	6.456577000	16.774311000
Mg	10.779322000	6.102500000	15.725132000
H	12.045637000	5.280416000	16.933905000
N	15.110731000	4.608979000	16.560296000
N	15.357399000	7.245844000	15.331233000
N	14.281067000	8.491713000	17.806728000
N	14.059724000	5.865220000	19.048828000
N	10.700813000	5.095788000	13.608317000
N	9.637438000	7.689294000	14.490301000
N	9.091955000	6.839640000	17.205436000
N	9.382307000	4.141727000	16.028603000

C	16.142712000	4.906096000	15.541620000
H	17.038806000	4.286201000	15.692168000
H	15.739395000	4.626127000	14.564398000
C	16.532913000	6.376816000	15.538150000
H	17.001110000	6.641765000	16.491053000
H	17.295165000	6.549643000	14.762933000
C	15.650126000	8.638663000	15.727746000
H	16.632685000	8.959655000	15.349561000
H	14.908587000	9.280328000	15.243853000
C	15.599934000	8.840363000	17.232035000
H	16.362127000	8.225812000	17.720091000
H	15.855848000	9.885679000	17.463634000
C	14.409836000	8.306357000	19.269205000
H	13.424644000	8.464030000	19.717071000
H	15.070506000	9.067511000	19.709496000
C	14.923602000	6.917824000	19.619371000
H	15.937424000	6.785078000	19.229472000
H	14.999069000	6.819803000	20.713125000
C	14.754744000	4.561275000	19.028300000
H	13.991260000	3.784358000	18.933305000
H	15.271737000	4.374692000	19.981904000
C	15.749656000	4.447254000	17.886109000
H	16.528938000	5.207927000	17.989706000
H	16.261283000	3.474747000	17.949704000
C	14.413416000	3.361914000	16.197532000
H	13.936778000	3.478492000	15.221509000
H	15.108455000	2.511356000	16.146568000
H	13.630069000	3.141720000	16.923274000
C	14.977977000	7.244062000	13.907426000
H	14.043502000	7.795331000	13.786863000
H	15.759079000	7.702931000	13.284297000
H	14.817980000	6.224076000	13.554597000
C	13.319751000	9.575839000	17.532973000
H	13.181867000	9.698671000	16.458276000
H	12.349380000	9.318375000	17.962248000
H	13.652922000	10.529737000	17.966547000
C	12.840028000	5.723537000	19.862843000
H	12.338588000	6.686932000	19.971400000
H	12.154435000	5.036680000	19.362698000
H	13.069820000	5.346186000	20.869686000
C	9.740433000	5.867009000	12.783982000
H	8.731263000	5.499375000	12.981337000
H	9.921328000	5.690784000	11.713469000
C	9.815182000	7.360113000	13.061140000
H	9.073709000	7.882012000	12.436792000
H	10.796593000	7.743257000	12.765446000
C	8.240234000	7.515058000	14.923678000
H	7.902652000	6.528308000	14.595332000
H	7.575517000	8.250771000	14.443072000
C	8.092102000	7.636884000	16.440140000
H	7.070530000	7.348502000	16.719277000
H	8.191760000	8.685685000	16.731492000
C	8.485345000	5.622522000	17.792456000
H	9.195537000	5.219756000	18.521235000
H	7.569879000	5.874227000	18.349050000
C	8.165912000	4.565284000	16.749459000
H	7.446481000	4.961858000	16.026656000
H	7.670853000	3.713529000	17.239528000
C	9.069747000	3.567154000	14.706515000
H	8.781383000	2.508241000	14.782705000
H	8.197243000	4.086745000	14.298919000
C	10.250339000	3.693801000	13.754141000
H	9.982773000	3.260859000	12.778313000
H	11.098088000	3.112736000	14.130975000
C	12.023174000	5.115207000	12.962146000
H	12.750865000	4.611492000	13.603379000
H	12.005575000	4.608133000	11.986611000
H	12.353765000	6.144457000	12.818698000
C	10.079184000	9.079157000	14.701221000
H	11.133980000	9.162509000	14.435106000
H	9.490574000	9.783741000	14.096230000
H	9.981249000	9.361483000	15.749850000

C	9.640217000	7.655648000	18.304883000
C	10.113956000	8.552829000	17.900824000
C	8.862356000	7.963675000	19.017820000
C	10.393489000	7.076414000	18.842869000
C	10.112912000	3.144949000	16.833162000
H	11.027208000	2.844166000	16.319719000
H	10.415054000	3.573038000	17.789295000
H	9.493445000	2.253830000	17.011943000
H	12.357728000	7.290122000	15.549899000

Monomer complex

Mg	13.791690000	6.430388000	16.914283000
H	12.165772000	6.204743000	16.357555000
N	15.206925000	4.681475000	16.528008000
N	15.215457000	7.369770000	15.402076000
N	14.206674000	8.434215000	17.924053000
N	14.193768000	5.744445000	19.050182000
C	16.138401000	5.059566000	15.442787000
H	17.077430000	4.490358000	15.504246000
H	15.673656000	4.781773000	14.493283000
C	16.445773000	6.553449000	15.448688000
H	16.997051000	6.817852000	16.357804000
H	17.108493000	6.791487000	14.602261000
C	15.485716000	8.764099000	15.815102000
H	16.447765000	9.120882000	15.418912000
H	14.716063000	9.399023000	15.368640000
C	15.468471000	8.923838000	17.332139000
H	16.295679000	8.359600000	17.776816000
H	15.639573000	9.981131000	17.587634000
C	14.352784000	8.205904000	19.378306000
H	13.359715000	8.280128000	19.828718000
H	14.963099000	8.990975000	19.848151000
C	14.956745000	6.839214000	19.684136000
H	15.987378000	6.795236000	19.315110000
H	15.010373000	6.701890000	20.775296000
C	14.989585000	4.498592000	19.000367000
H	14.291239000	3.659593000	18.944197000
H	15.568911000	4.355953000	19.924256000
C	15.928930000	4.468014000	17.799063000
H	16.686307000	5.253530000	17.896855000
H	16.472885000	3.510687000	17.787755000
C	14.441100000	3.478672000	16.144118000
H	13.863356000	3.687061000	15.241251000
H	15.102858000	2.619962000	15.962620000
H	13.727611000	3.212694000	16.925657000
C	14.615178000	7.346425000	14.053058000
H	13.674471000	7.900783000	14.062239000
H	15.289254000	7.785715000	13.304087000
H	14.379990000	6.323095000	13.756130000
C	13.098807000	9.375487000	17.665183000
H	12.962776000	9.520927000	16.592322000
H	12.167005000	8.957583000	18.051706000
H	13.281821000	10.352801000	18.133886000
C	12.920495000	5.505196000	19.759047000
H	12.313404000	6.411810000	19.774508000
H	12.344908000	4.744103000	19.228257000
H	13.090567000	5.176735000	20.794161000

References

- [1] J. Coates, D. Hadi, S. Lincoln, *Aust. J. Chem.* **1982**, *35*, 903-909.
- [2] D. Schuhknecht, C. Lhotzky, T. P. Spaniol, L. Maron, J. Okuda, *Angew. Chem. Int. Ed.* **2017**, *56*, 12367-12371.
- [3] U. Wannagat, H. Autzen, H. Kuckertz, H.-J. Wismar, *Z. Anorg. Allg. Chem.* **1972**, *394*, 254-262.
- [4] a) A. Causero, G. Ballmann, J. Pahl, H. Zijlstra, C. Färber, S. Harder, *Organometallics* **2016**, *35*, 3350-3360; b) L. E. Lemmerz, V. Leich, D. Martin, T. P. Spaniol, J. Okuda, *Inorg. Chem.* **2017**, *56*, 14979-14990; c) A. Marcó, R. Compañó, R. Rubio, I. Casals, *Microchimica Acta* **2003**, *142*, 13-19.
- [5] E. Merck, *Komplexometrische Bestimmungsmethoden mit Titriplex Merck*, Darmstadt, 1975.
- [6] J. Intemann, J. Spielmann, P. Sirsch, S. Harder, *Chem. Eur. J.* **2013**, *19*, 8478-8489.
- [7] a) C. R. Noller, *J. Am. Chem. Soc.* **1931**, *53*, 635-643; b) C. R. Noller, W. R. White, *J. Am. Chem. Soc.* **1937**, *59*, 1354-1356.
- [8] S. Harder, F. Feil, T. Repo, *Chem. Eur. J.* **2002**, *8*, 1991-1999.
- [9] M. C. Burla, R. Caliendo, M. Camalli, B. Carrozzini, G. L. Cascarano, L. De Caro, C. Giacovazzo, G. Polidori, D. Siliqi, R. Spagna, *J. Appl. Crystallogr.* **2007**, *40*, 609-613.
- [10] G. M. Sheldrick, *Acta Crystallogr. A* **2008**, *64*, 112-122.
- [11] L. J. Farrugia, *J. Appl. Crystallogr.* **2012**, *45*, 849-854.
- [12] D. Schuhknecht, C. Lhotzky, T. P. Spaniol, L. Maron and J. Okuda, *Angew. Chem. Int. Ed.*, **2017**, *56*, 12367-12371.
- [13] W. Fegler, A. Venugopal, T. P. Spaniol, L. Maron and J. Okuda, *Angew. Chem. Int. Ed.*, **2013**, *52*, 7976-7980.
- [14] H. Putz, K. Brandenburg, *Diamond - Crystal and Molecular Structure Visualization, Crystal Impact*, Bonn, 2017.
- [15] Gaussian 09, Revision D.02, M. J. Frisch, G. W. Trucks, H. B. Schlegel, G. E. Scuseria, M. A. Robb, J. R. Cheeseman, G. Scalmani, V. Barone, B. Mennucci, G. A. Petersson, H. Nakatsuji, M. Caricato, X. Li, H. P. Hratchian, A. F. Izmaylov, J. Bloino, G. Zheng, J. L. Sonnenberg, M. Hada, M. Ehara, K. Toyota, R. Fukuda, J. Hasegawa, M. Ishida, T. Nakajima, Y. Honda, O. Kitao, H. Nakai, T. Vreven, J. A. Montgomery, Jr., J. E. Peralta, F. Ogliaro, M. Bearpark, J. J. Heyd, E. Brothers, K. N. Kudin, V. N. Staroverov, R. Kobayashi, J. Normand, K. Raghavachari, A. Rendell, J. C. Burant, S. S. Iyengar, J. Tomasi, M. Cossi, N. Rega, J. M. Millam, M. Klene, J. E. Knox, J. B. Cross, V. Bakken, C. Adamo, J. Jaramillo, R. Gomperts, R. E. Stratmann, O. Yazyev, A. J. Austin, R. Cammi, C. Pomelli, J. W. Ochterski, R. L. Martin, K. Morokuma, V. G. Zakrzewski, G. A. Voth, P. Salvador, J. J. Dannenberg, S. Dapprich, A. D. Daniels, O. Farkas, J. B. Foresman, J. V. Ortiz, J. Cioslowski, D. J. Fox, Gaussian, Inc., Wallingford CT, 2009.
- [16] A. D. Becke, *J. Chem. Phys.* **1993**, *98*, 5648.
- [17] J. P. Perdew, Y. Wang, *Phys. Rev. B* **1992**, *45*, 13244.
- [18] (a) A. D. McLean, G. S. Chandler, *J. Chem. Phys.* **1980**, *72*, 5639. (b) W. J. Hehre, R. Ditchfield, J. A. Pople, *J. Chem. Phys.* **1972**, *56*, 2257.
- [19] S. Grimme, S. Ehrlich, L. Goerigk, *J. Comp. Chem.* **2011**, *32*, 1456-1465.
- [20] (a) A. E. Reed, L. A. Curtiss, F. Weinhold, *Chem. Rev.* **1988**, *88*, 899. (b) F. Weinhold, In *The Encyclopedia of Computational Chemistry* (Eds.: Schleyer, P. v. R.), John Wiley & Sons, Chichester, pp 1792, 1998.